AD-A074 261 KAMAN AVIDYNE BURLINGTON MA F/G 1/3
AN EVALUATION OF THE ADINA FINITE ELEMENT PROGRAM FOR APPLICATI--ETC(U)
FEB 79 T R STAGLIANO, L J MENTE DNA001-78-C-0057
UNCLASSIFIED KA-TR-162 DNA-4876F NL

1 OF 1
AD A074261

END
DATE FILMED
10-79
DDC

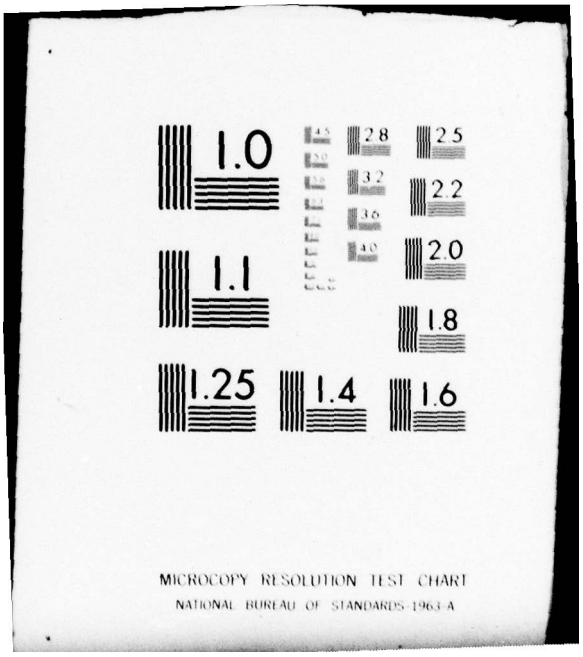
1.0
1.1
1.25
1.4
1.6
1.8
2.0
2.2
2.5
2.8
3.2
3.6
4.0
MICROCOPY RESOLUTION TEST CHART
NATIONAL BUREAU OF STANDARDS-1963-A

(12) LEVEL III

DNA 4876F

AN EVALUATION OF THE ADINA FINITE ELEMENT PROGRAM FOR APPLICATION TO AIRCRAFT OVERPRESSURE VULNERABILITY

Kaman AviDyne
Division of Kaman Sciences Corp.
83 Second Avenue
Northwest Industrial Park
Burlington, Massachusetts 01803

February 1979

Final Report for Period 12 November 1977—31 October 1978

CONTRACT No. DNA 001-78-C-0057

APPROVED FOR PUBLIC RELEASE;
DISTRIBUTION UNLIMITED.

THIS WORK SPONSORED BY THE DEFENSE NUCLEAR AGENCY
UNDER RDT&E RMSS CODE B342078464 N99QAXAJ50201 H2590D.

Prepared for
Director
DEFENSE NUCLEAR AGENCY
Washington, D. C. 20305

Destroy this report when it is no longer needed. Do not return to sender.

PLEASE NOTIFY THE DEFENSE NUCLEAR AGENCY, ATTN: STTI, WASHINGTON, D.C. 20305, IF YOUR ADDRESS IS INCORRECT, IF YOU WISH TO BE DELETED FROM THE DISTRIBUTION LIST, OR IF THE ADDRESSEE IS NO LONGER EMPLOYED BY YOUR ORGANIZATION.

UNCLASSIFIED (18) DNA, SBIE

SECURITY CLASSIFICATION OF THIS PAGE (When Data Entered)

(19) **REPORT DOCUMENTATION PAGE**

READ INSTRUCTIONS BEFORE COMPLETING FORM

1. REPORT NUMBER: DNA 4876F, AD-E300 579
2. GOVT ACCESSION NO.
3. RECIPIENT'S CATALOG NUMBER (9)

4. TITLE (and Subtitle): (6) AN EVALUATION OF THE ADINA FINITE ELEMENT PROGRAM FOR APPLICATION TO AIRCRAFT OVERPRESSURE VULNERABILITY.

5. TYPE OF REPORT & PERIOD COVERED: Final Report for 12 Nov 77—31 Oct 78

6. PERFORMING ORG. REPORT NUMBER: (14) KA-TR-162

7. AUTHOR(s): (10) Thomas R. Stagliano, Lawrence J. Mente

8. CONTRACT OR GRANT NUMBER(s): (15) DNA 001-78-C-0057

9. PERFORMING ORGANIZATION NAME AND ADDRESS: Kaman AviDyne, Division of Kaman Sciences Corp., 83 Second Avenue, Northwest Industrial Park, Burlington, Massachusetts 01803

10. PROGRAM ELEMENT, PROJECT, TASK AREA & WORK UNIT NUMBERS: (16) Subtask N99QAXAJ502-01

11. CONTROLLING OFFICE NAME AND ADDRESS: (11) Director, Defense Nuclear Agency, Washington, DC 20305

12. REPORT DATE: Feb 1979

13. NUMBER OF PAGES: 80

14. MONITORING AGENCY NAME & ADDRESS (if different from Controlling Office): (12) 81p.

15. SECURITY CLASS (of this report): UNCLASSIFIED

15a. DECLASSIFICATION/DOWNGRADING SCHEDULE

16. DISTRIBUTION STATEMENT (of this Report)

Approved for public release; distribution unlimited. (17) J502

17. DISTRIBUTION STATEMENT (of the abstract entered in Block 20, if different from Report)

62704H

18. SUPPLEMENTARY NOTES

This work sponsored by the Defense Nuclear Agency under RDT&E RMSS Code B342078464 N99QAXAJ50201 H2590D.

19. KEY WORDS (Continue on reverse side if necessary and identify by block number)

Aircraft Vulnerability
Digital Computer Program
Overpressure Effects
Finite Element Method
Structural Response Analysis
Elastic-Plastic Material

20. ABSTRACT (Continue on reverse side if necessary and identify by block number)

In aircraft overpressure vulnerability, stiffened thin-walled panel configurations are subjected to surface pressure loadings of varying time histories. These dynamic loads subject the impinged structural components to large deflections and an elastic-plastic material response. The ability to predict accurately the deflection and strain time histories of complex aircraft structures of arbitrary geometry has become of increasing importance.

DD FORM 1 JAN 73 1473 EDITION OF 1 NOV 65 IS OBSOLETE

UNCLASSIFIED

SECURITY CLASSIFICATION OF THIS PAGE (When Data Entered)

194 970

20. ABSTRACT (Continued)

The ADINA (Automatic Dynamic Incremental Nonlinear Analysis) computer code is evaluated to determine if it is a numerically accurate, computationally efficient means of analyzing these complex structures under transient pressure loading. In this initial evaluation, the ADINA solutions for clamped beams, simply supported, and clamped flat unstiffened panels and flat stiffened panels subjected to transient pressure loadings are compared with solutions from other nonlinear structural codes, presently used in aircraft vulnerability calculations, which are based on finite difference and modal methods of analysis.

The ADINA 2-D beam elements and 3-D isoparametric continuum elements are evaluated for these dynamic nonlinear structural problems. Furthermore, comparisons in accuracy and computational efficiency are made using these elements in which the various spatial and temporal numerical solution techniques embodied in the ADINA program were exercised. Thus, for example, tradeoffs between equilibrium iterations and updating the stiffness matrix are evaluated for both the total and updated Lagrangian formulations. The numerical accuracy is examined by a comparison of converged predictions of transient strains and deflections with the solutions from the other nonlinear structural codes. The computational efficiency is based on central processor (C.P.) time for solutions obtained on a CDC 6600 computer.

ADINA was found to be an efficient and accurate computer code which provides the full nonlinear capability required for aircraft vulnerability analysis. Shortly, a new version of ADINA will be available that contains a desirable thin shell element. However, ADINA finite elements would still have to be extended to include various shaped stringer and frame cross sections and multilayered skin configurations associated with aircraft structures.

PREFACE

This report was prepared for the Defense Nuclear Agency (DNA) under Contract Number DNA001-78-C-0057 by Kaman AviDyne, Burlington, MA. Captain J. M. Rafferty of DNA was project officer and Mr. Lawrence J. Mente was project leader for Kaman AviDyne. The authors wish to acknowledge Mr. William N. Lee for his work in setting up and updating the ADINA program on the CDC 6600 computer. This work was performed in the Structural Mechanics Section of Kaman AviDyne headed by Mr. Emanuel S. Criscione.

Conversion factors for U.S. customary to metric (SI) units of measurement.

To Convert From	To	Multiply By
angstrom	meters (m)	1.000 000 X E -10
atmosphere (normal)	kilo pascal (kPa)	1.013 25 X E +2
bar	kilo pascal (kPa)	1.000 000 X E +2
barn	meter^2 (m^2)	1.000 000 X E -28
British thermal unit (thermochemical)	joule (J)	1.054 350 X E +3
calorie (thermochemical)	joule (J)	4.184 000
cal (thermochemical)/cm^2	mega joule/m^2 (MJ/m^2)	4.184 000 X E -2
curie	*giga becquerel (GBq)	3.700 000 X E +1
degree (angle)	radian (rad)	1.745 329 X E -2
degree Fahrenheit	degree kelvin (K)	$t_K = (t°f + 459.67)/1.8$
electron volt	joule (J)	1.602 19 X E -19
erg	joule (J)	1.000 000 X E -7
erg/second	watt (W)	1.000 000 X E -7
foot	meter (m)	3.048 000 X E -1
foot-pound-force	joule (J)	1.355 818
gallon (U.S. liquid)	meter^3 (m^3)	3.785 412 X E -3
inch	meter (m)	2.540 000 X E -2
jerk	joule (J)	1 000 000 X E +9
joule/kilogram (J/kg) (radiation dose absorbed)	Gray (Gy)	1.000 000
kilotons	terajoules	4.183
kip (1000 lbf)	newton (N)	4.448 222 X E +3
kip/inch^2 (ksi)	kilo pascal (kPa)	6.894 757 X E +3
ktap	newton-second/m^2 ($N-s/m^2$)	1.000 000 X E +2
micron	meter (m)	1 000 000 X E -6
mil	meter (m)	2.540 000 X E -5
mile (international)	meter (m)	1.609 344 X E +3
ounce	kilogram (kg)	2.834 952 X E -2
pound-force (lbs avoirdupois)	newton (N)	4.448 222
pound-force inch	newton-meter (N·m)	1.129 848 X E -1
pound-force/inch	newton/meter (N/m)	1.751 268 X E +2
pound-force/foot^2	kilo pascal (kPa)	4.788 026 X E -2
pound-force/inch^2 (psi)	kilo pascal (kPa)	6.894 757
pound-mass (lbm avoirdupois)	kilogram (kg)	4.535 924 X E -1
pound-mass-foot^2 (moment of inertia)	kilogram-meter^2 ($kg·m^2$)	4.214 011 X E -2
pound-mass/foot^3	kilogram/meter^3 (kg/m^3)	1.601 846 X E +1
rad (radiation dose absorbed)	**Gray (Gy)	1.000 000 X E -2
roentgen	coulomb/kilogram (C/kg)	2.579 760 X E -4
shake	second (s)	1.000 000 X E -8
slug	kilogram (kg)	1.459 390 X E +1
torr (mm Hg, 0° C)	kilo pascal (kPa)	1.333 22 X E -1

*The becquerel (Bq) is the SI unit of radioactivity; 1 Bq = 1 event/s.
**The Gray (Gy) is the SI unit of absorbed radiation.

A more complete listing of conversions may be found in "Metric Practice Guide E 380-74," American Society for Testing and Materials.

TABLE OF CONTENTS

LIST OF ILLUSTRATIONS

LIST OF TABLES

SECTION 1
INTRODUCTION

In analyzing nuclear overpressure effects on aircraft structures, the techniques have increased in the level of sophistication through several stages of development. Initially, in Reference 1, static solutions of simple flat plates and straight and circular beams coupled with dynamic load factors were used to assess the dynamic response of individual aircraft structural elements, such as stringers, frames and panels, to overpressure loading. The next step in sophistication was accomplished in the development of the computer code NOVA (Reference 2), which predicted the dynamic response of individual structural elements, represented by straight or curved beams and flat and cylindrical thin panels, to the transient pressure loads associated with the blast wave from a nuclear burst. These analyses included both geometric and physical nonlinearities inherent in the behavior of these structural elements in the response range bounded by threshold of permanent damage and catastrophic damage. Further sophistication was introduced recently through the computer code NOVA-2S (Reference 3), which can analyze stiffened panels. The discrete stiffeners can be placed on either surface of the flat or the cylindrical panels in either coordinate direction, for both elastic and inelastic deformations.

The current stiffened panel formulation in NOVA-2S has limitations in geometry and boundary conditions when applied to the larger complex aircraft substructures. For this reason the nonlinear finite element computer program ADINA (Reference 4) is evaluated herein for possible future improvement of the response analysis to determine aircraft vulnerability to overpressure. The initial selection of ADINA over several other nonlinear finite element codes, such as MARC and ANSYS, was primarily based on obtaining a source deck of a finite element computer program of good analytical quality at a reasonable cost. It should be noted that all the fully nonlinear finite element computer codes considered are proprietary codes which restrict the operation of the computer program to the organization purchasing the code. The use of these codes is also available through Control Data's CYBERNET system.

ADINA presently has the capability of performing linear and nonlinear, static or dynamic analyses of two or three-dimensional complex structures in which both geometrical and physical nonlinearities can be included. The current version of ADINA contains several finite element types; namely, truss elements, two-dimensional plane stress or strain elements, three-dimensional solid elements and beam elements. Shortly, the final version of ADINA will be available and will include a thin shell element which is important to aircraft structural analysis.

During this evaluation the three-dimensional solid element was used as a substitute for the thin shell element at the cost of some computational efficiency to model the skin of unstiffened and stiffened panels. The beam element was used to model uniform beams and panel stiffeners. Response comparisons were made with other nonlinear structural codes used in the NOVA evaluation in Reference 2. With the three-dimensional solid elements it was not practical to model a complex aircraft-type structure for demonstration purposes. Thus, the primary emphasis for this ADINA computer code evaluation was to determine if the code is a numerically accurate, computationally efficient means of analyzing these dynamic structural response problems to a transient pressure loading.

Section 2 of this report presents a general description of the ADINA computer code. The structural response applications and evaluations of ADINA are given in Section 3. Section 4 presents the conclusions and recommendation based on these evaluations.

SECTION 2
DESCRIPTION OF THE ADINA COMPUTER CODE

ADINA (Automatic Dynamic Incremental Nonlinear Analysis) is a general purpose linear and nonlinear, static and dynamic three-dimensional finite element analysis program. The users' manual of the program is presented in Reference 4 and the theory and numerical techniques involved in the program can be found in more detail in References 5 through 7. The ADINA code is derived from the NONSAP (Reference 8) and SAP IV (Reference 9) computer programs. This section summarizes the general capabilities and methods incorporated into the ADINA program as contained in the ADINA documentation.

Using ADINA, a discrete representation of a structural system may be established by a model composed of combinations of several different finite elements. The current ADINA program contains truss elements, beam elements, isoparametric plane stress and strain elements and isoparametric solid or thick shell elements. An element is isoparametric if the nodal points define both the geometry and the finite element analysis points, and if the shape (interpolation) functions defining geometry and the unknown displacements are the same. The isoparametric elements are generally more effective in practical analyses than the generalized coordinate finite element models. Thus, fewer isoparametric elements are required for an accurate solution than generalized coordinate elements. The final version of ADINA to be released shortly will include a new thin shell element that is needed for efficient aircraft structural modelling. All of the isoparametric elements allow the user a choice of nodal locations, and provide both vertex and interior nodes. The nodal patterns, nonlinear formulations and material models for these various finite elements available in ADINA are summarized in Figures 1 through 5 obtained from Reference 10.

Two nonlinear formulations are available in ADINA which have been termed total Lagrangian and updated Lagrangian. The option to use both formulations is available for all finite elements, except for the truss and beam elements for which only the updated Lagrangian is used.

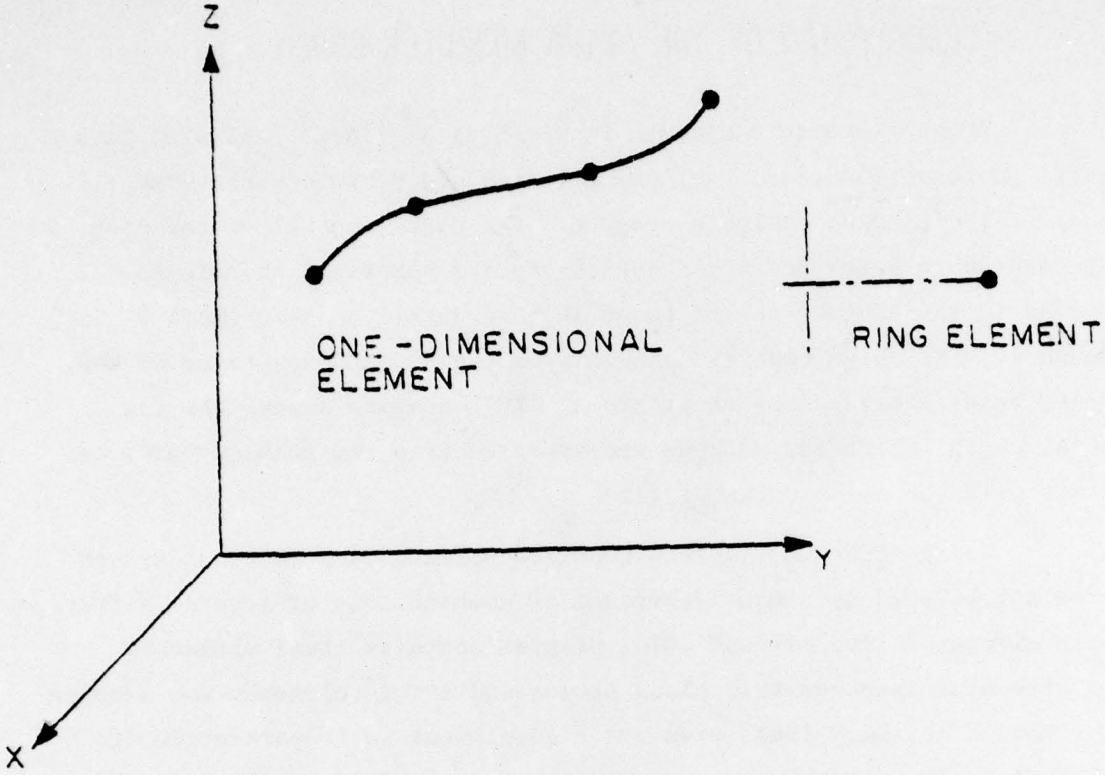

AVAILABLE NONLINEAR FORMULATIONS

a. LINEAR ANALYSIS

b. MATERIALLY NONLINEAR ONLY

c. UPDATED LAGRANGIAN WITH LARGE DISPLACEMENTS BUT SMALL STRAINS

AVAILABLE MATERIAL MODELS

a. LINEAR ELASTIC

b. NONLINEAR ELASTIC

c. THERMO-ELASTIC

d. ISOTHERMAL PLASTICITY (PERFECTLY-PLASTIC, ISOTROPIC OR KINEMATIC STRAIN HARDENING)

e. THERMO-ELASTIC-PLASTIC AND CREEP

Figure 1.* Truss Element

*Obtained from Reference 10.

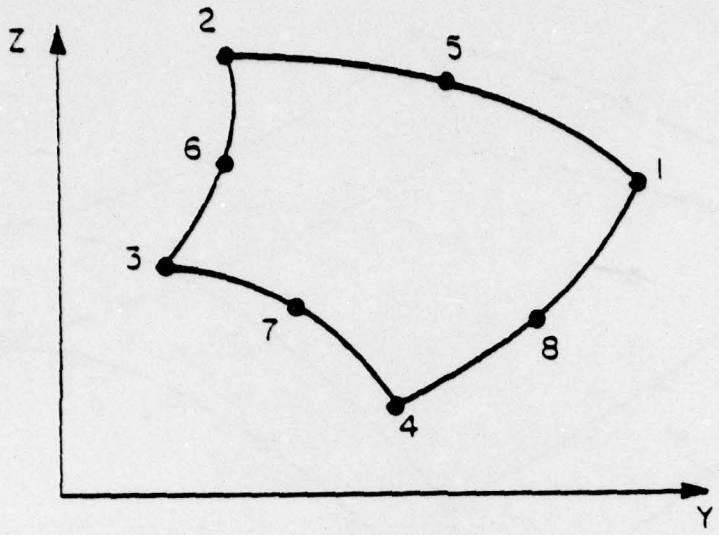

AVAILABLE
NONLINEAR FORMULATIONS

a. LINEAR ANALYSIS
b. MATERIALLY NONLINEAR ONLY
c. UPDATED LAGRANGIAN
d. TOTAL LAGRANGIAN

AVAILABLE
MATERIAL MODELS

a. ISOTROPIC LINEAR ELASTIC
b. ORTHOTROPIC LINEAR ELASTIC
c. ISOTROPIC THERMO-ELASTIC
d. CURVE DESCRIPTION NONLINEAR MODEL
e. CAP MODEL
f. CONCRETE MODEL
g. ISOTHERMAL PLASTICITY, VON MISES YIELD CONDITION (ISOTROPIC OR KINEMATIC HARDENING)
h. THERMO-ELASTIC-PLASTIC AND CREEP, VON MISES YIELD CONDITION (ISOTROPIC OR KINEMATIC HARDENING)
i. ISOTROPIC NONLINEAR ELASTIC, INCOMPRESSIBLE (MOONEY-RIVLIN MATERIAL) (plane stress only)

Figure 2.* Two-dimensional plane stress, plane strain and axisymmetric solid elements.

*Obtained from Reference 10.

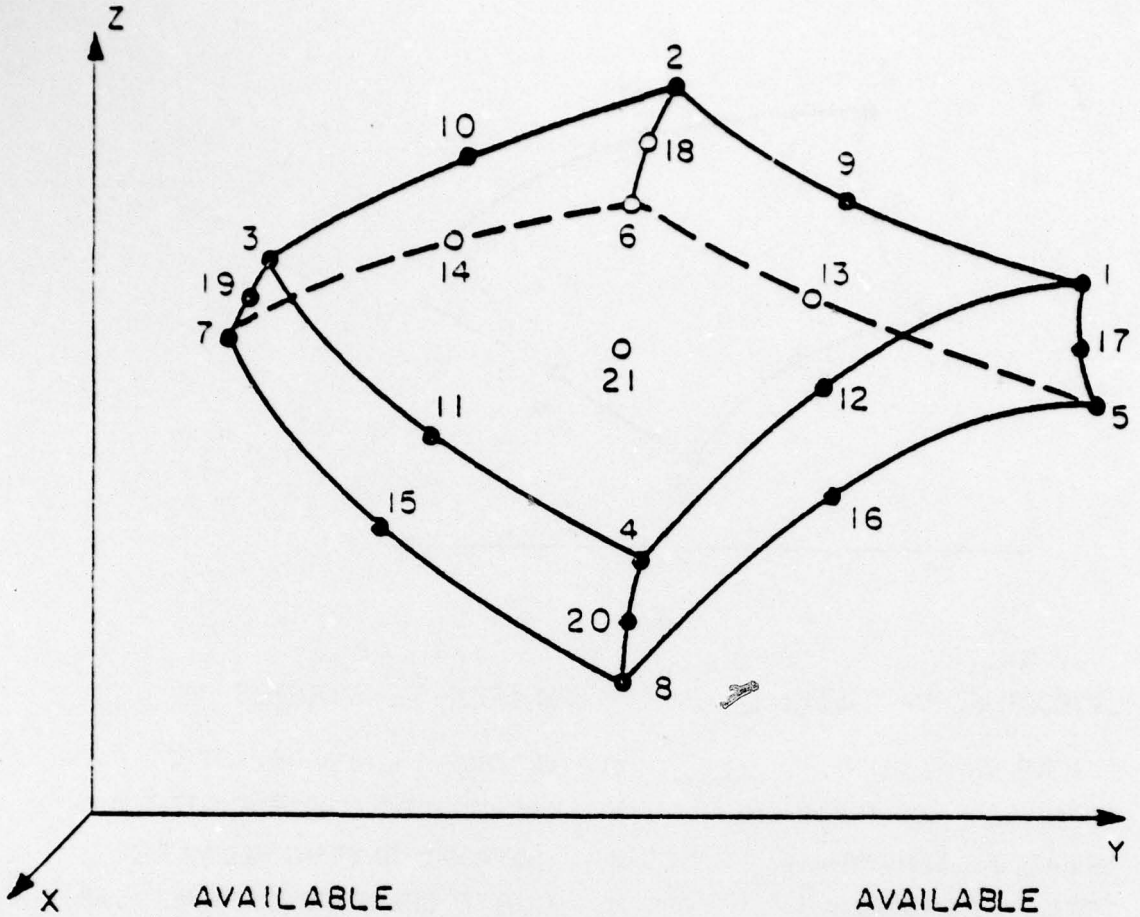

AVAILABLE NONLINEAR FORMULATIONS

a. LINEAR ANALYSIS
b. MATERIALLY NONLINEAR ONLY
c. UPDATED LAGRANGIAN
d. TOTAL LAGRANGIAN

AVAILABLE MATERIAL MODELS

a. ISOTROPIC LINEAR ELASTIC
b. ORTHOTROPIC LINEAR ELASTIC
c. ISOTROPIC THERMO-ELASTIC
d. CURVE DESCRIPTION NON-LINEAR MODEL
e. CAP MODEL
f. CONCRETE MODEL
g. ISOTHERMAL PLASTICITY, VON MISES YIELD CONDITION (ISOTROPIC OR KINEMATIC HARDENING)
h. THERMO-ELASTIC-PLASTIC AND CREEP, VON MISES YIELD CONDITION (ISOTROPIC OR KINEMATIC HARDENING)

Figure 3.* Three-dimensional solid and thick shell element.

*Obtained from Reference 10.

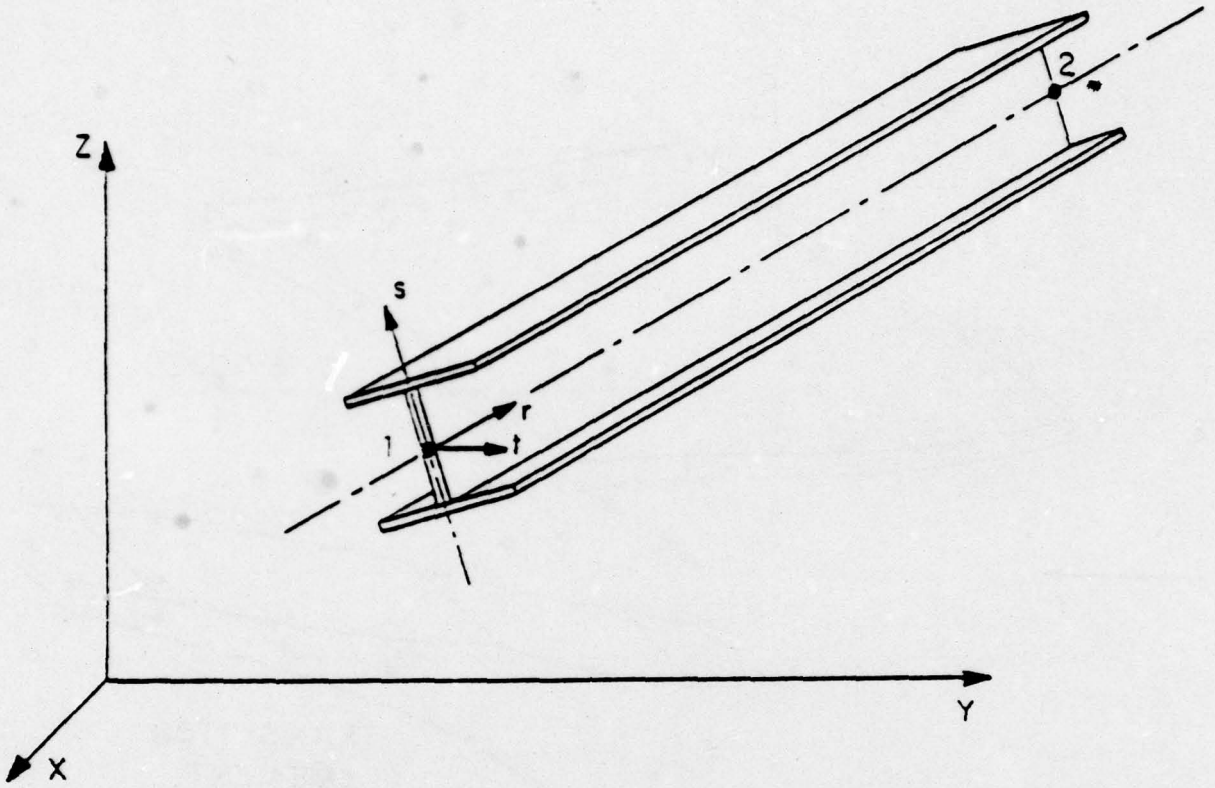

AVAILABLE
NONLINEAR FORMULATIONS

a. LINEAR ANALYSIS

b. MATERIALLY NONLINEAR ONLY

c. UPDATED LAGRANGIAN WITH LARGE DISPLACEMENTS BUT SMALL STRAINS

AVAILABLE
MATERIAL MODELS

a. ISOTROPIC LINEAR ELASTIC

b. ISOTHERMAL PLASTICITY (PERFECTLY-PLASTIC OR ISOTROPIC STRAIN HARDENING, RECTANGULAR AND PIPE SECTION)

Figure 4.* Three-dimensional beam element.

*Obtained from Reference 10.

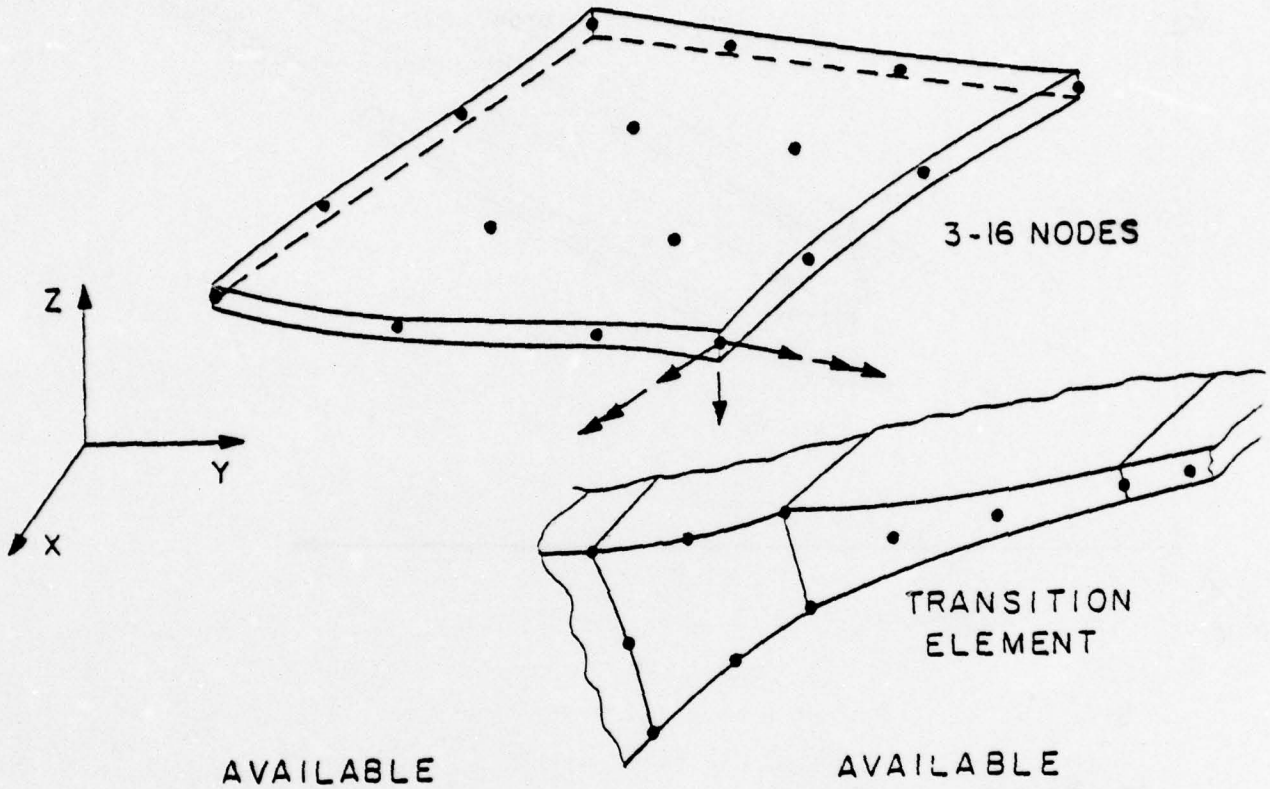

AVAILABLE
NONLINEAR FORMULATIONS

a. LINEAR ANALYSIS

b. MATERIALLY NONLINEAR ONLY

c. UPDATED LAGRANGIAN

d. TOTAL LAGRANGIAN

AVAILABLE
MATERIAL MODELS

a. ISOTROPIC LINEAR ELASTIC

b. ISOTHERMAL PLASTICITY, VON MISES YIELD CONDITION (ISOTROPIC OR KINEMATIC HARDENING)

Figure 5.* Thin shell element (variable-number-nodes).

*Obtained from Reference 10.

Both formulations are based on the same procedures; but in the total Lagrangian solution scheme all static and kinematic variables are referred to the initial configuration at zero time, while for the updated Lagrangian these variables are referred to the configuration at current time t. The difference between the total or updated Lagranian formulations is found in their relative numerical effectiveness which is dependent on the finite element and the constitutive relations that are employed. These formulations include large displacements and large strain effects for all finite elements, except for the small strain assumption used in the truss, beam and thin shell elements. In ADINA, for the two-dimensional plane stress or strain elements, the three-dimensional solid elements and the future thin shell elements, the updated Lagrangian can only be used for linear elastic materials, whereas the total Lagrangian can be used for both linear and nonlinear material conditions.

Various material models are available for the different elements as indicated in Figures 1 through 5; however, for aircraft structural response to overpressure the linear elastic and isothermal plasticity models are of most interest. The isothermal plasticity model is based on the von Mises yield condition for both isotropic and kinematic strain hardening. The elastic-plastic material model assumes a bilinear representation of the stress-strain curve of the material.

The structural response of the finite element representation of the real structure is calculated in ADINA using an incremental solution of the equations of equilibrium. In dynamic analyses the temporal integrations can be performed either by explicit or implicit methods. The central difference method is used for the explicit time integration while either the Newmark method or the Wilson method is employed in the implicit time integration. The incremental dynamic equilibrium equations for an assemblage of finite elements are given as follows, using explicit time integration,

$$M\ddot{U}^t + C\dot{U}^t = R^t - F^t \qquad (1)$$

and using implicit time integration

$$M\ddot{U}^{t+\Delta t} + C\dot{U}^{t+\Delta t} + K^{t}U = R^{t+\Delta t} - F^{t} \qquad (2)$$

where

$\ddot{U}$ = vector of nodal point accelerations

$\dot{U}$ = vector of nodal point velocities

$U = U^{t+\Delta t} - U^{t}$ = vector of nodal point displacement increments

M = mass matrix

C = damping matrix

K = tangent stiffness matrix

R = external load vector

F = vector of nodal point forces equivalent to the element stresses

t, $t+\Delta t$ superscripts indicate evaluation at times t and $t+\Delta t$

For the implicit time integration formulation of Equation (2), it is generally necessary to use equilibrium iteration and to update the linear effective stiffness matrix at preselected time steps. The trade-off involved in obtaining the best mix between equilibrium iterations and stiffness updates for solution accuracy and computational efficiency is considered in Section 3.

Either a lumped mass or consistent mass matrix may be specified in ADINA; however, for the explicit time integration method only the lumped mass matrix is used. Concentrated masses corresponding to selected degrees of freedom can be specified in ADINA.

In ADINA the external loading can consist of concentrated nodal point forces and surface pressure loading. The surface pressure loading is defined spatially for each surface element by specifying pressure values at the four corner nodes. The pressure intensities at positions on the surface of the element are obtained by linear interpolation of the specified corner values. For transient loadings the time function is defined by discrete values of concentrated force or pressure specified at selected values of time. Loads at intermediate times are determined by linear interpolation. The arrival time of the loading function can also be specified. The initial conditions for the finite element system in terms of displacement, velocity and acceleration can be specified for all active degrees of freedom.

The ADINA program is an out-of-core solver of the equilibrium equations and very large finite element systems can be considered. The structural matrices are stored in compacted form as one-dimensional arrays and only the elements below the "skyline" of the matrices are processed. The amount of low-speed storage required to store all information pertaining to each block of finite elements will govern the size of the finite element system that can be considered. ADINA has the capability of obtaining response solutions in terms of displacements, stresses and strains for both static and transient loading conditions. Furthermore, an eigensolution routine using the determinant search method is incorporated into ADINA for calculating the frequencies and mode shapes of the structural model.

SECTION 3
ADINA RESPONSE COMPARISONS AND EVALUATION

In the past a primary application of the ADINA code was to aid in the design of nuclear power generating plants. Therefore, ADINA has been extensively used to analyze thick-wall structures, concrete materials, and soil-structure interactions. Thus, in the development of ADINA the beam and thin shell elements were the last to be added to the finite element library, where the thin shell element will be available shortly. The ADINA code therefore has not been widely used for the transient response analysis of beams and thin walled plates or shells which are basic structural elements found in aircraft structures. Aircraft construction is typified by a thin skin reinforced by stringers, longerons, and frames for the fuselage, and spars and ribs covered by thin skin (unstiffened and stiffened) for lifting surfaces.

This section presents an evaluation of ADINA finite element models for three types of idealized structural members; namely, a doubly clamped beam, a simply-supported or fully clamped square thin panel, and a simply-supported or fully clamped square stiffened thin panel (a combination of the first two structural components). Each of these components is subjected to an idealized blast-wave loading and only the first cycle of the structural dynamic response is monitored during which the component generally becomes fully plastic and experiences significant permanent set. In this evaluation the ADINA response results are compared with the responses generated from other nonlinear structural codes based upon different methods of analysis.

Previously, two structural response codes have been utilized by Kaman AviDyne for the dynamic analysis of severe blast-wave loading upon aircraft structural elements; the NOVA code composed of DEPROB (beam analysis) and DEPROP (unstiffened and stiffened panel analysis) given in References 3 and 11 and PETROS 3 or 3.5 (References 12 and 13). These codes are used to predict the deflection and strain transient responses for the idealized beam and plate structures and to provide a set of data to be used as a basis for comparison with the ADINA predictions.

The ADINA modeling of each structure is varied by element mesh size, integration point mesh, timewise finite difference operator, stiffness matrix updating, the frequency of equilibrium iterations and the time step size. Comparisons are made among the various modelings based on the accuracy of the transient displacment and strain prediction (at the center of each structure) and the central processor time required to analyze a one cycle response. All ADINA solutions were performed on the same CDC 6600 computer and all the DEPROB, DEPROP and PETROS 3 and 3.5 solutions were run on the same or an equivalent computing machine.

3-1 STRUCTURAL RESPONSE COMPUTER CODES USED FOR COMPARISON.

This subsection gives a brief description of the two structural response codes used to generate a data base for correlation with the ADINA predictions.

3-1.1 NOVA-2S: DEPROB and DEPROP.

The NOVA-2S (Nuclear Overpressure Vulnerability Analysis Version 2 Stiffened Panel) computer program (References 2 and 3) uses the DEPROB and DEPROP structural dynamic routines to analyze the response of beams and unstiffened or stiffened panels to an arbitrary blast wave.

DEPROB (Dynamic Elastic Plastic Response of Beams) was developed for use with stringers, longerons, frames, and ribs. This is a finite difference code and is based on a method developed at MIT (References 14 and 15). The beam is divided into a series of discrete masses interconnected by straight weightless bars and the beam response is computed at each mass point. The cross section is idealized by a set of discrete points called flanges. For plastic analysis each flange is subdivided into a set of mechanical sublayers which allow kinematic hardening (in the uniaxial sense) to occur. The numerical integration of the second-order dynamic response differential equations uses the central difference formulation.

DEPROP (Dynamic Elastic Plastic Response of Panels) is based on the Novozhilov nonlinear strain-displacement relations for large displacement response of thin panels based on the assumption of undeformable normals. The inelastic formulation is based on the Mises-Hencky

yield surface, a kinematic hardening model and the Hencky stress-strain relation from the deformation theory of plasticity. An assumed modal solution is used to determine the surface displacements. The numerical spatial integration is performed by the Simpson's quadrature formula along the surface of the panel and the Legendre-Gauss quadrature formula for integration through the panel thickness. The temporal solution is advanced by a central difference operator and therefore the time step size is governed by a stability criterion.

3-1.2 PETROS.

PETROS 3 and 3.5 (References 12 and 13) are MIT computer programs to predict the large deflection, elastic-plastic transient responses of arbitrary initial shape thin shells under arbitrary initial velocity distribution and transient loads. This is a finite difference code using a central difference operator for both spatial and temporal integrations. Both PETROS 3 and PETROS 3.5 were exercised on the sample panel problems, and the structural response predictions of PETROS 3.5 (the latest version of the two codes) compares favorably with the PETROS 3 predictions. All further reference to the PETROS code will be confined to the PETROS 3 version.

3-2 STRUCTURAL RESPONSE OF BEAMS.

As a simple verification of the applicability of ADINA to blast-wave-loading structural response analysis, a correlation study was undertaken with ADINA predictions and an experimental data base generated at MIT (References 14 and 15). Table 1 summarizes the geometric and material properties of a doubly clamped aluminum beam. Approximately twenty percent of the central beam span was subjected to a high explosive blast wave. For modeling purposes a triangular shaped time varying force (Figure 6) is used to represent the "impulsive" loading of the explosives cemented directly on the beam surface. The duration of the forcing function is derived from the detonation wave velocity through the explosive material and the function's amplitude is calculated to achieve the same total impulse in the model as was experienced during the experiment.

Table 1.* Geometrical and physical properties of beam.

	Beam 111 (Ref. 14)
Material Properties	Aluminum 6061-T6
E, psi	10.7×10^6
σ_o, psi	41200
E_t, psi	61200
ρ, lb/in^3	0.097
Length, in	10.0
Thickness, in	0.242
Width, in	1.195
Total Impulse, psi-sec	0.2724
Initial Velocity, ft/sec	4480
Length of Charge, in (centered on C_L)	1.988
Edge Conditions	Clamped
Measured Permanent Set, in	0.522

*From Reference 2.

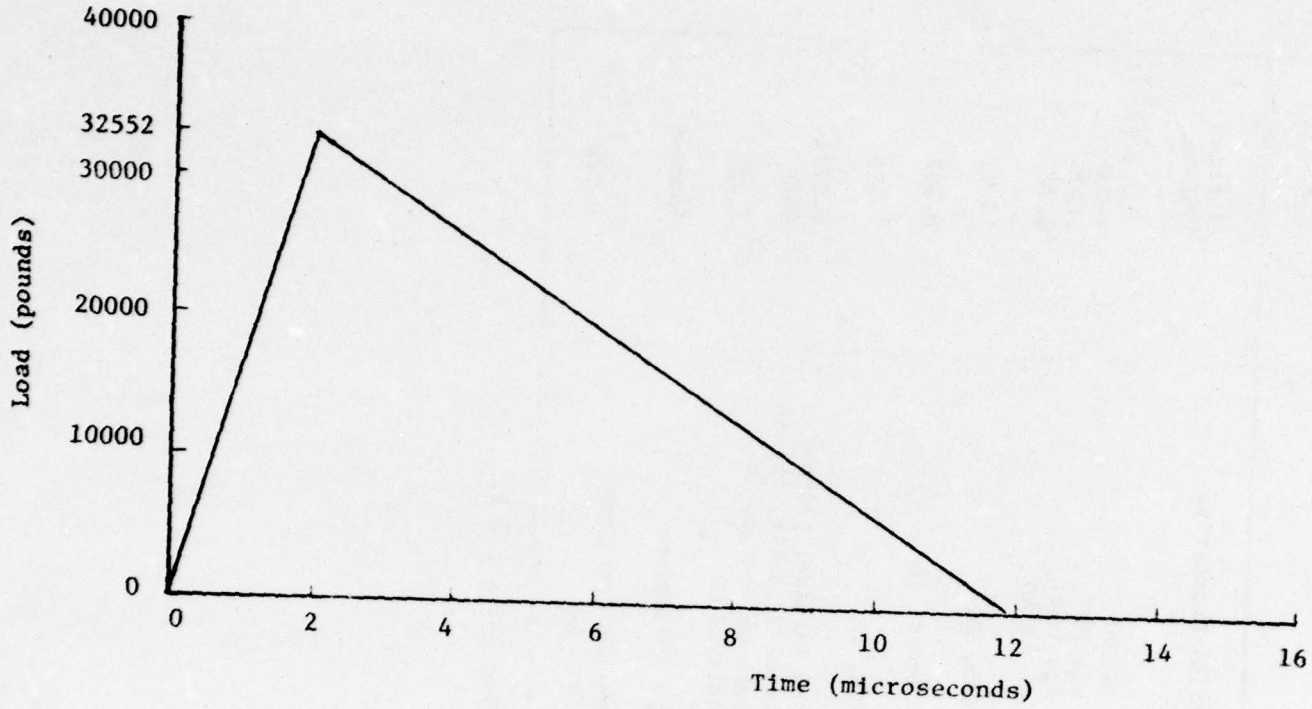

Figure 6. Load versus time - blast wave approximation for MIT beam.

3-2.1 ADINA Modeling for Beams.

Ten three-dimensional beam elements (Reference 16, Figure 5) are used to model the half span of the experimental beam with a clamped boundary at one end and a symmetry condition imposed at the second end. The large geometric deflections and material deformations apparent from the experiment required the use of the updated Lagrangian formulation (Reference 17) for the finite element solution. In this formulation all the material and geometric quantities are referred back to their value at the last time instant of the solution. This formulation is actually a strict Lagrangian formulation advanced through time (using a material description of the deformation process) and not an Eulerian formulation, which while based on the present deformation state is actually a spatial description of the deformation process, References 18 and 19.

The ADINA solution process for the large deformation analysis of beams is influenced by three main factors:

1) The choice of the temporal finite difference operator. There are three operators available to the user, the explicit central difference formulation and the implicit Wilson-θ and Newmark methods. The Newmark method is more flexible and more widely utilized than the Wilson-θ method and will be used for comparisons with the more classically used central difference method.

2) The spatial integration point mesh used for the numerical solution of the differential equations. The beam elements are restricted to the use of Newton-Cotes operator and the choice of mesh size is important in terms of accuracy and solution time.

3) The actual step by step timewise solution procedure. The user may specify the cycles at which the material stiffness matrix is to be updated and the cycles at which a force equilibrium iteration is to be performed.

It should be noted that for the implicit time integration formulation (conventional ADINA formulation), References 17 and 20, the tangent stiffness matrix can be updated during the solution process to give a more accurate solution. In addition, the implicit solution at time $t + \Delta t$ is based on the extrapolated nodal forces from time t (see equation 2, Section 2). The accuracy of the solution can vary considerably because of this approximation, especially if the Newmark temporal operator is used with a large time step size (Δt). Therefore equilibrium iterations performed periodically during the solution process will increase the accuracy of the solution.

In the explicit time integration formulation shown in equation 1 in Section 2 (unconventional ADINA formulation, References 17 and 20), the tangent stiffness matrix is included in the nodal force vector F (no updating is required) and the nodal force vector is not extrapolated (no equilibrium iterations are necessary). The time step size (Δt) is restricted by a central difference stability criterion based on the highest natural frequency ω_{max} of the discretized system:

$$\Delta t \leq \frac{1.6}{\omega_{max}} \tag{3}$$

For thin beams modeled with a lumped mass matrix ω_{max} can be approximated by:

$$\omega_{max} \cong \frac{2}{\ell} \sqrt{\frac{E}{\rho}} \tag{4}$$

where ℓ = <u>smallest</u> element length (in)
E = material Young's modulus (psi)
ρ = material density (lb-sec^2/in^4)

The value $\sqrt{\frac{E}{\rho}}$ is the approximate longitudinal wave velocity through the material. For most structural materials (steel, alumimum, titanium and nickel) this velocity is approximately the same (200,000 in/sec). Thus for thin beam structural dynamic analysis the finite element mesh size will determine the maximum allowable solution time step size. Note that this approximation is valid only if the beam thickness is less than one-half the <u>element</u> length. If the beam is thicker than this value (the

finite element mesh becomes too refined) the highest natural frequency of the discretized structure will become dependent on the beam bending stiffness and not the longitudinal wave speed. The approximation of ω_{max} for a lumped mass model becomes

$$\omega_{max} \cong \frac{4h}{\ell^2}\sqrt{\frac{E}{\rho}} \tag{5}$$

where h equals the beam thickness and ω_{max} varies as the inverse square of the smallest element length.

The central difference operator may be CPU time consuming on the computer for many structural dynamics problems; however, when a blast wave loading is analyzed the time duration associated with the load application is very short compared to the fundamental structural period and for these problems the central difference formulation may be cost effective.

3-2.2 Response Comparisons for Various Solutions.

Figure 7 presents a comparison among four different ADINA runs, a DEPROB (Reference 2) calculation and the experimental midspan deflection data (Reference 14) for the MIT doubly clamped aluminum beam 111 (Reference 14). All of the ADINA calculations were performed with a time step size of two microseconds and both the Newmark and the central difference temporal operators were used. Another calculation using a Δt = 1 μsec was made with the central difference operator and this essentially duplicated the two microsecond calculation and demonstrated that a stable solution had been obtained. (It should be noted that given an element length of 0.5 in., the central difference stability criterion of equations 3 and 4 specifies a time step of two microseconds for stability.) Table 2 summarizes all of the ADINA and DEPROB calculations for the clamped beam. Several parameters are indicated for comparison: time step size, temporal operator, number of cycles between updates of the material stiffness matrix (K) and number of cycles between equilibrium iterations (E) (K/E is not applicable for the explicit central difference operator), integration point mesh (Newton-Cotes), CPU time for a 1500 μsec solution run, and peak midspan deflection. It is immediately apparent

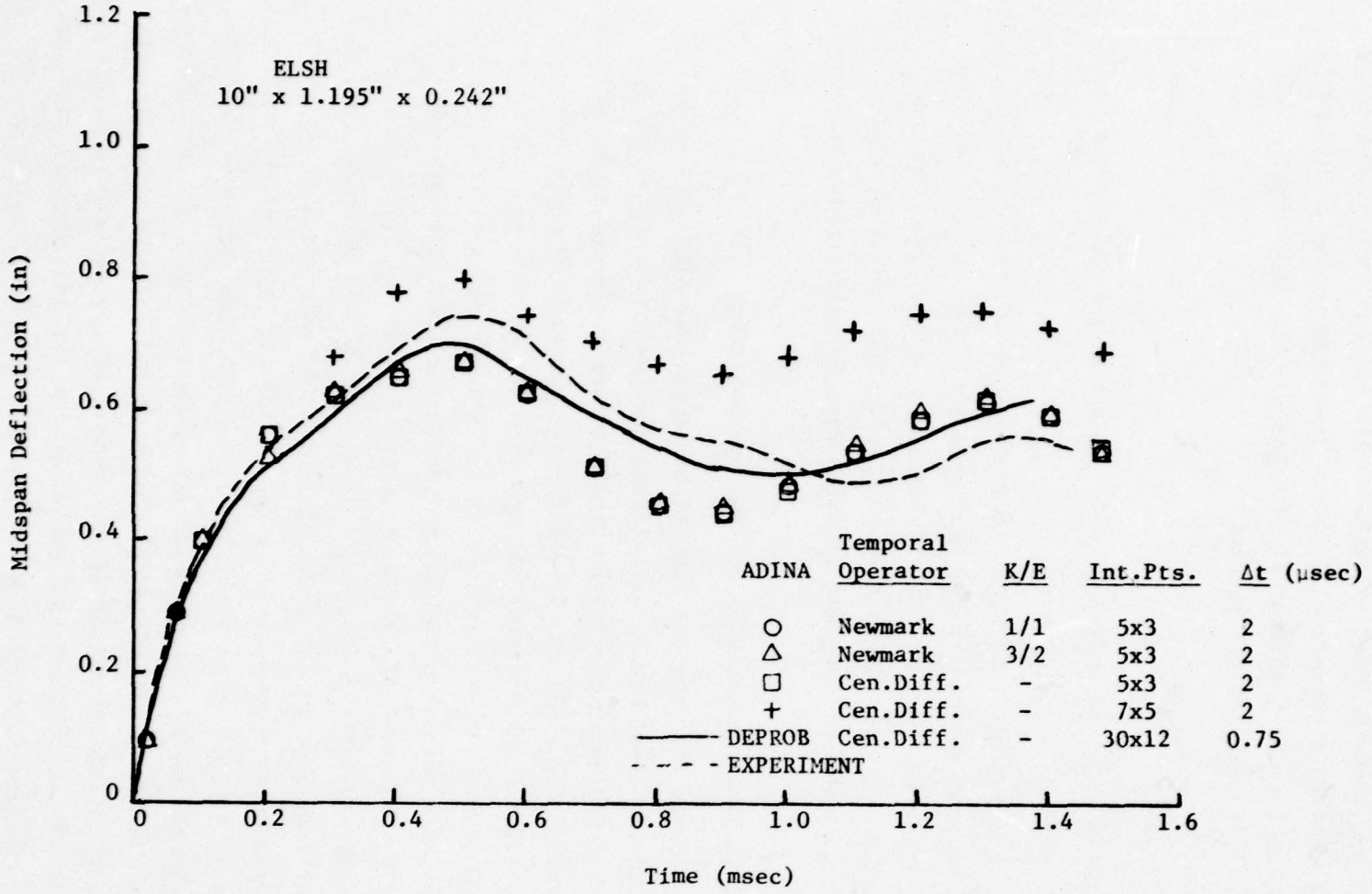

Figure 7. Deflection versus time profle for the midspan of the MIT beam.

Table 2. Comparisons of numerical predictions for the MIT beam 111.

Numerical Code	Time Step (Δt) Size (micro-Seconds)	Temporal Operator	K/E (Cycles)	Integration Mesh	Solution Time (cpu) sec	Peak[+] Deflection (in)
ADINA[*]	2	Newmark	1/1	5x3x1	570	0.674
	2	Newmark	1/1	5x3x1	565	0.674
	2	Newmark	10/3	5x3x1	Diverged	-
	2	Newmark	3/2	5x3x1	300	0.675
	2	Newmark	1/0	5x3x1	Diverged	-
	2	Central Diff.	-	5x3x1	135	0.676
	2	Central Diff.	-	7x5x1	270	0.799
	1	Central Diff.	-	7x5x1	1/2 run 280	0.801
	4	Newmark	1/0	5x3x1	Diverged	-
DEPROB	0.75	Central Diff.	30 masses/half beam		175	0.698

[*]ADINA model included ten elements/half beam.

[+]Experimental peak deflection was 0.74 in.

All numerical predictions included an elastic strain hardening material model.

K/E is value in cycles for:

K = cycles between updating stiffness matrix

E = cycles between equilibrium iterations

K = E = 0 = no updates or iterations

that for the ADINA runs attempted, the central difference operator produces a solution with a reduced CPU time compared to the Newmark operator. This is typical for structural dynamic analyses in which the fundamental loading period of the forcing function is of the same magnitude as the smallest natural period of the discretized structure.

The implicit time operators become cost effective when the time step size utilized is much greater than that required for the central difference operator. The implicit operators generally require a significant amount of stiffness updating and force equilibrium iterations which are numerically time consuming. The implicit operators also require more matrix manipulations for the same solution steps because the conventional formulation is utilized rather than the unconventional formulation (see equations (1) and (2)). These additional computational costs necessitate the use of a time step size approximately four times the central difference stability limit for the implicit Newmark operator to be cost effective (based on CPU time).

Among the predictions made with the Newmark operator, it is noted that the variation of the K/E parameter (cycles between updating the stiffness matrix/cycles between equilibrium iterations) resulted in marked differences in the solution CPU time and the predicted peak midspan deflection. From Table 2 and Figure 7 it is shown that the response predictions are identical for the Newmark operator with K/E values of 3/2 and 1/1 and the central difference operator (all with integration meshes of 5 x 3 x 1). The solutions with K/E equal to 1/0 and 10/3 diverged, where each solution run used the same time step of two microseconds. This implies that equilibrium iterations are necessary to achieve a stable solution and that a minimum number of iterations and material stiffness matrix updates are needed for a converged, stable solution.

From Table 2 it is apparent that a time step size of five microseconds with the Newmark operator is comparable in solution CPU time with the central difference operator and a time step of two microseconds. The ADINA prediction with K/E of 10/3 should have given a

comparable solution time; however, this prediction did not converge. The inherent reason for the difficulty in utilizing the implicit operator economically is the applied loading duration. The load is experimentally applied for only four microseconds (based on the explosive's detonation wave speed); therefore, to accurately model the loading pulse as a triangular load/time history, a time step size one half of the pulse duration is required which is the same length as the central difference stability limit of two microseconds. The central difference operator is usually the most convenient and the most economical to use, for "impulsive" blast loading.

Finally, from Table 2 and Figure 7, the differences in deflection response associated with a change in the integration point mesh utilized for the numerical solution is to be discussed. A five by three integration mesh in the bending plane of the beam was used in most of the ADINA models shown in Figure 7, except for one case using a seven by five mesh to check the predictive accuracy. The seven by five mesh produced a beam response that is significantly larger than the experimentally measured midspan displacements.

The ADINA code utilizes a Newton-Cotes integration formulation (References 5, 16, 21) in order to provide an equally spaced mesh and to provide integration points at all of the element surfaces (a closed Newton-Cotes formulation). The Newton-Cotes formulation uses n + 1 points to exactly integrate a function of order n or less. For the nonlinear beam elements presented in Reference 16, a cubic interpolation function is utilized for all the displacements along the neutral axis and if transverse shear effects are neglected a linear interpolation function is used for the two transverse directions. The Newton-Cotes integration scheme requires five points to integrate along the neutral axis for the cubic interpolation function, and for nonlinear analysis at least three points are required along the direction that defines the plane of bending to accurately include the material plasticity. However, the Newton-Cotes integration function does not monotonically converge upon a solution value. Hildebrand, Reference 21, demonstrates that the

best mesh size for a Newton-Cotes formulation might be five ordinates because the errors associated with successive formulas of higher order (finer mesh size) oscillate with increasing amplitude about the true value. Another factor that will affect the accuracy of the prediction compared to the experimental data is the order of the actual displacement variation along the beam's neutral axis during the early loading stages of response. The detonation wave and ensuing plastic wave will create "hinges" or "kinks" in the material and during the passage of these waves the cubic interpolation function will inadequately model the local displacement field. However, this is only a momentary effect at each beam location creating small inaccuracies in predicting the peak deflection response, and it should not affect the prediction of the permanent beam deformation. Figure 7 shows that all of the predictions (DEPROB, ADINA with 5 x 3 mesh) are approaching the experimental "long duration" permanent deflection except for the ADINA prediction with the 7 x 5 integration mesh. This observation tends to support Hildebrand's findings that the higher order Newton-Cotes formulations may oscillate about the actual solution and that a fully converged numerical solution may require a significantly larger number of integration ordinates.

Reviewing the numerical predictions tabulated in Table 2 and plotted in Figure 7, it appears that the modeling with the central difference operator, a two microsecond time step, and a five by three point integration mesh provides the most accurate and cost effective ADINA solution. This ADINA modeling also compares favorably with the DEPROB analysis (0.75 microsecond time step and a central difference operator). It should be pointed out that no strain prediction comparisons were performed because strains are not a current output quantity for the ADINA program. Private communication with the authors of the ADINA code have indicated that strain information can be easily obtained for the beam element but this needs to be demonstrated. Additionally, the ADINA modeling for nonlinear analysis restricts the beam cross section to be initially rectangular or circular. This presents a major problem when a plasticity analysis is to be performed for an arbitrarily shaped stiffener, such as I, Z or T sections. At this time the ADINA program can accurately

and economically predict the large deflection and large plastic strain deformation of a simple beam structure, but is not capable of easily analyzing an actual aircraft beam-like structure.

3-3 STRUCTURAL RESPONSE OF PLATES.

A more significant application of the ADINA finite element code is the elastic-plastic large deflection analysis of stiffened or unstiffened thin plates. These types of structural components are analogous to the standard semi-monocoque aircraft structural elements and the analysis of these planar structures can be used to evaluate the applicability of ADINA to aircraft overpressure vulnerability studies.

An idealized plate structure was selected for this ADINA evaluation in order to conform to a previous comparison (Reference 2) conducted with DEPROP and PETROS 3. The assumed model consists of a square aluminum plate twenty inches on each side and a uniform 0.1 in thickness. The plate has an assumed uniform continuous boundary condition of either perfectly clamped or held-simply-supported. Table 3 summarizes the geometric and material properties of the idealized square plate. The stiffened plate is represented by the same basic plate described above plus a single uniform stiffener materially identical to the plate and located along one central meridian. Table 3 includes the stiffener geometric information.

These idealized plate structures are loaded by a uniform linearly decaying pressure pulse. The total pulse duration is 2000 microseconds (Figure 8) and the time history of the pressure pulse is a linear representation of a blast-shock wave overpressure load on a structural component. The load is applied for a longer duration than the analyzed structural response (1500 microseconds). The response predictions are carried out for a sufficient time to allow peak deflections and strains to be obtained and, additionally, to allow one cycle of post-peak-deformation structural response. The characteristic pressure load initial amplitude (P_m) is problem dependent. For a purely elastic response P_m is equal to 100 psi, for an elastic-plastic response the value of P_m depends on the geometry as follows:

Table 3. Plate geometry and material.

PLATE

Geometry: Length = 20 in.
Width = 20 in.
Thickness = 0.1 in.

Material: Aluminum

Modulus of Elasticity = 1×10^7 psi

Poisson's Ratio = 0.3 ELPP

Yield Stress = 40000 psi

Strain Hardening Slope = 150,000 psi ELSH

STIFFENER

Geometry: One stiffener located on plate lower surface.
Stiffener is at plate center parallel to one principal direction.
Length = 20 in.
Thickness = 1.5 in.
Width = 0.4 in.

Material: Aluminum

Modulus of Elasticity = 1×10^7 psi

Poisson's Ratio = 0.3

Yield Stress = 40000 psi

Specimen	Boundary Condition	P_m (psi)
Unstiffened Plate ELPP, ELSH	Simply-Sup.	200
	Clamped	250
Stiffened Plate ELPP	Simply-Sup.	250
	Clamped	350
Unstiffened Plate Elastic	Clamped	100

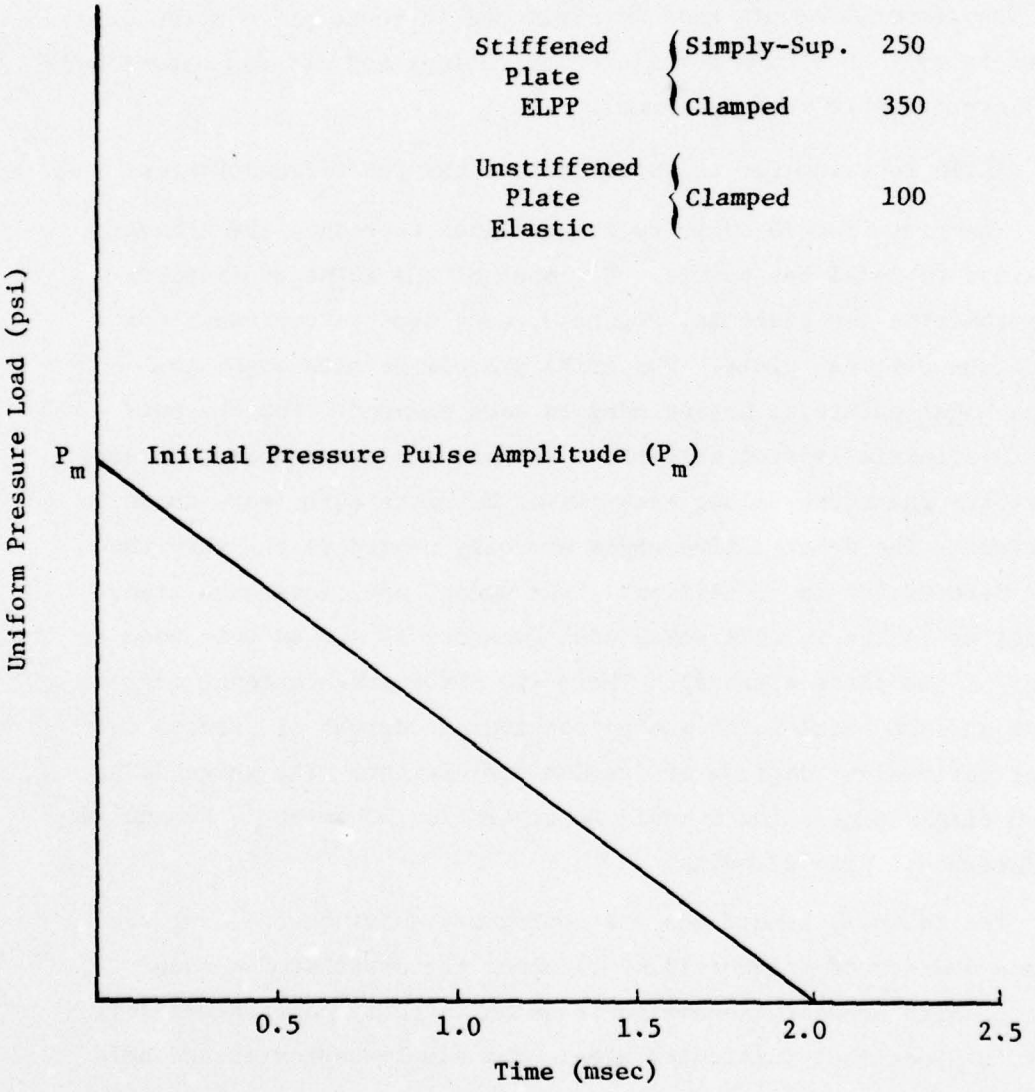

Figure 8. Uniform pressure pulse time history for all the analyzed plate models.

Geometry	P_m (psi)
Simply-Supported, Unstiffened	200
Clamped, Unstiffened	250
Simply-Supported, Stiffened	250
Clamped, Stiffened	350

These load levels were selected to achieve a structural response that produced large deflections (ratio of normal deflection to plate thickness of about 30) and substantial permanent strains (about 9-10%). The response levels that were reached in these plate structures correspond to typical ultimate failure deflections and strains experienced in actual overpressure test specimens.

3-3.1 ADINA Modeling for the Stiffened or the Unstiffened Plates.

The plate double symmetry was utilized to reduce the element mesh required to model the panels. For most of the ADINA predictions nine isoparametric 3-D elements, Figure 3, were used to represent one quarter of the original plate. The ADINA program permits eight to twenty-one nodal points to be included in each element. For the purposes of this initially flat thin-plate analysis, sixteen nodes, located at each vertex and midway along each planar boundary edge, were found to be sufficient. The deleted five nodes are only needed if the thru-the-thickness deformation is significant (four nodes, one along each transverse edge) or if the initial structural geometry is curved (one node at the center of the plate element). There are three translational degrees of freedom at each nodal point and no rotational degrees of freedom for a total of forty-eight degrees of freedom per element. The three nodes along each planar edge allow a cubic interpolation function to be applied for the internodal displacements.

The boundary conditions are approximated by constraining the appropriate degrees of freedom (d.o.f.) along the associated element edges. A clamped boundary condition is established by constraining all the d.o.f.'s along that particular edge. The simply-supported and held boundary condition is defined by constraining two of the translational

d.o.f.'s along the edge of one surface and constraining only the d.o.f. normal to the plate along the edge of the opposite surface. For this analysis the d.o.f.'s along the y edge (for example, assuming x and y define the element plane and that the z direction is normal to the element) would have the x and z d.o.f. constrained along the lower surface and only the z d.o.f. constrained along the upper surface of the edge. At a vertex all of the d.o.f.'s would be constrained at the node on the lower surface. This is an articifical means of providing a simply supported and held boundary condition, but is necessary when rotational degrees of freedom are not included at the element nodes.

The ADINA code provides three material models for the description of the material plasticity. The material is permitted to be elastic perfectly plastic (ELPP) or the material can be described by two elastic strain hardening (ELSH) models. One strain hardening model is based on an isotropic hardening law and the other uses a kinematic hardening rule. The yield condition in ADINA is based on the von Mises yield criteria and is used for all three material models. In this study all three plasticity models are utilized, however, the kinematic ELSH model was inhibited by a programming error which was corrected by the ADINA authors late in this study. It should be noted that in the correlation comparisons for the ELSH plate material response, the DEPROP code (Reference 2) utilizes a kinematic hardening model and the PETROS 3 code (Reference 12) uses a mechanical sublayer model of which the kinematic model is a subset.

The solution procedures developed in ADINA are based on either a total or an updated Lagrangian formulation. For the beam analysis discussed in Section 3-2 the updated Lagrangian formulation was utilized exclusively. However, for the three dimensional continuum element both formulations are provided in the ADINA program, but only the total Lagrangain formulation can be used for a material nonlinear analysis. Comparison between the two formulations by the ADINA authors show no computational differences and demonstrate a slight improvement in computational efficiency for the updated Lagrangian formulation. The

total Lagrangian formulation is the more "classical" of the two formulations. It is apparent that when the ADINA program was established the authors had more confidence in the use of the total Lagrangian formulation for the general response of a three dimensional element and restricted the code to this formulation. It is not known whether future versions of ADINA will include the updated Lagrangian formulation for all material models.

The timewise finite difference operator used for these plate models was restricted to the implicit Newmark formulation. The practical use of the explicit central difference operator was eliminated by a stability criterion which is dependent upon the highest natural frequency (ω_{max}) of the discretized structure. The value of ω_{max} is dependent upon the velocity of the longitudinal and the transverse waves through the material and the size of the finite element mesh (similar to the discussion in Section 3-2 for the "one dimensional" beam). However the use of a three dimensional continium element to model a thin plate creates an artifically large ω_{max} that is dependent upon the plate thickness. This ω_{max} causes the time step size (Δt) required for stability to be orders of magnitude smaller than an appropriate Δt for the implicit Newmark operator. This restriction on the use of the central difference operator for plate analysis would be removed if a thin plate element (instead of a three dimensional element) were used for the geometrical model. The use of the implicit Newmark operator for these plate models allows the time step size, the number of cycles between updating the stiffness matrix (K) and the number of cycles between force equilibrium iterations (E) to be designated as variables in analyzing the comparative accuracy and efficiency of the ADINA program.

The finite element formulation requires the use of a spatial numerical integration scheme to solve the relevant differential equations. The three-dimensional element uses a Gaussian integration formulation along all three element directions. The Gaussian formulation of order n can exactly integrate a polynomial of order 2n-1. The three-dimensional element in the ADINA program is assumed to have a single major plane and

a minor normal to this plane referred to as the element thickness. The integration point grid used in the element is identical for both directions in the major plane and can be different for the thickness direction. This provision is ideal for a plate analysis in which the interpolation function along the plate's principal directions are cubic and there is no appreciable deformation through the plate thickness. A cubic interpolation function for the displacement requires a minimum of two Gaussian points for exact integration. However, the strain is a quadratic function of the displacements; therefore, it is conceivable that four Gaussian points will be required for complete and exact integration of the strains along the plate's principal directions. For a purely membrane response, only one Gaussian station is required through the thickness; however, due to material nonlinearity and plate bending, from two to four Gaussian points are needed through the thickness.

The use of a sufficient number of Gaussian points to exactly integrate the strain relations has been disputed in the finite element literature (References 22 and 23) for three-dimensional elements used to approximate thin panels. The three-dimensional element automatically includes a functional dependency of the strain energy density on the element's tranverse shear. If the aspect ratio (element length to thickness) becomes too large, an artificially large amount of transverse shear is included in the numerical predictions. The "classical" method for relieving this restriction is to under integrate, or to use a sufficient number of integration points to integrate exactly the displacements but to integrate approximately the strain relations. This is a theoretically inconsistent but an empirically proven means of using three-dimensional elements to model thin plate structural geometries. The "appropriate" number of integration points for both the planar direction and the through-the-thickness direction is one subject of comparison in Section 3-3.2.

In summary, the basic plate geometry is modeled by nine isoparametric three-dimensional finite elements taking advantage of the plate's double symmetry (one comparison includes a prediction with

twenty-five elements). The elements each contain sixteen nodal points and each nodal point is defined by three translational degrees of freedom. The material plasticity is modeled by either an ELPP or an isotropic ELSH model, both of which utilize the von Mises yield criteria. The Newmark temporal operator is used exclusively and the basic time step size is the theoretical central difference stability limit. Variations of the time step size and cycles between stiffness matrix updates and cycles between equilibrium iterations are studied. The spatial numerical integrations are performed with a Gaussian integration formulation and the number of points in the integration grid is varied. The studies are duplicated for both simply-supported and clamped boundary conditions. Once an accurate and computationally efficient ADINA modeling has been established, an additional evaluation is conducted for stiffened plates.

Stiffened plates (or panels) are common geometrical configurations for thin light-weight aircraft structures. The stiffeners are approximated by three-dimensional beam elements (see Figure 4 and Section 3-2) attached along a central meridional nodal line of the plate. Six beam elements are used (one between each nodal point) as the stiffener model for both the clamped and simply supported plates and are attached to nodes on the lower surface (load is applied to the upper surface).

For the clamped plate, the boundary constraints remain the same in either the stiffened or the unstiffened configuration. The simply-supported and held edge was modeled by constraining the two edge-normal degrees of freedom at the nodes on the lower surface edge and only constraining the plate normal degree of freedom at edge nodes on the upper surface. The rotational degree of freedom about the planar direction normal to the beam elements (at all nodes along the beam) is allowed to be arbitrary for beam bending.

The beam elements use the updated Lagrangian formulation (the only formulation provided), a Newmark temporal operator for consistency with the plate elements and a 5 x 3 x 1 integration grid as discussed in Subsection 3-2. The time step size and cycle dependent parameters are

constrained to be the same for both the plate elements and the beam elements. Conveniently, the highest natural frequency of the beam elements places a "central difference" stability limit of 3.7 microseconds on the time step size used for the beam elements. This compares favorable with the basic 3 microsecond limit used for the plate elements and allows a not too inefficient utilization of the Newmark operator with the beam element.

The beam elements are attached to the lower surface nodes of the plate model, however the current ADINA program does not allow a nodal offset. With no offset the center of the beam elements is attached to the plate node which places one-half of the stiffener below the plate and approximately one-half of the stiffener on the upper surface of the plate. This slightly alters the elastic bending stiffness of the stiffened plate but more radically affects the plastic response of the stiffener material. It should be noted for comparative purposes: 1) the DEPROP (Reference 2) code includes a stiffener offset so that the stiffener can be properly modeled as being on the lower surface of the plate, 2) PETROS 3 (Reference 12) does not allow stiffeners.

3-3.2 Plate Response Comparisons for Various Solutions.

Tables 4 and 5 and Figures 9 and 10 show comparisons among ADINA, DEPROP and PETROS 3 predictions of a simply-supported or clamped (respectively) unstiffened plate for an assumed idealized blast-wave loading (Figure 8). In the tables and the figures the variables under investigation are the time step size (Δt), K/E (number of solution cycles between updating the material tangent stiffness matrix/number of cycles between force equilibrium iteration), and integration point mesh. These variables are compared based on solution accuracy (deflection and strain predictions) and computational efficiency (CPU time on a CDC 6600 computer).

It is noted in Table 4 that, for an ADINA solution with the Newmark temporal operator, a periodical updating of the material tangent stiffness matrix is required. All four predictions without any stiffness

Table 4. Numerical predictions of a simply supported unstiffened ELPP plate subjected to blast wave loading.

Numerical Method	Timestep Δt (μsec)	K/E[4] (Cycles)	Integration Pts	Solution CPU Time (sec)	Peak Defl. (in)	Peak Strain (%)
ADINA[1]	3	0/0	4x4x2	1000	2.15	4.11
	3	0/0	2x2x4	570	2.32	4.07
	3	0/3	2x2x4	735	3.19	12.50
	3	1/0	2x2x4	3630	2.82	7.06
	3	1/0	2x2x2	2525	2.82	6.90
	3	0/1	2x2x4	1020	2.40	4.9
	3	1/0	4x4x2	5830	2.60	7.50
	1.5	1/0	2x2x2	5075	2.82	6.93
	3	1/3	2x2x2	2610	2.82	6.9
	3	10/3	2x2x4	1005	2.81	7.0
	9	3/2	2x2x4	615	2.80	6.90
	9	10/2	2x2x4	350	2.73	6.40
	9	3/1	3x3x3	1055	2.60	7.27
	9	3/1	3x3x4	1290	2.60	7.30
	9	3/1	4x4x4	2160	2.59	7.56
	15	2/2	2x2x4	Diverged	-	-
	15	10/3	2x2x4	Diverged	-	-
DEPROP[2]	3.0	25 modes	16x16x5	1725	2.83	8.88
PETROS 3[3]	1.5		20x20x5	2870	2.83	6.86

(1) Reference 4

(2) Reference 2

(3) Reference 12

(4) K/E is value in cycles for:

K = cycles between updating stiffness matrix

E = cycles between equilibrium iterations

K = E = 0 = no updates or iterations

Table 5. Numerical predictions of a clamped unstiffened ELPP plate subjected to blast wave loading.

Numerical Method	Timestep Δt (sec)	K/E (Cycles)	Integration Pts	Solution CPU Time (sec)	Peak Defl. (in)	Peak Strain (%)
ADINA (9 elements)	3	3/1	2x2x4	1800	3.20	9.3
	3	5/2	2x2x4	1250	3.20	9.3
	9	3/1	2x2x4	630	3.18	9.2
	3	5/2	3x3x4	2510	2.73	7.95
	3	1/0	4x4x2	6495	2.73	7.92
	9	3/1	4x4x4	2150	2.72	7.92
ADINA (25 elements)	3	5/2	2x2x4	6495	3.24	11.03
DEPROP	3	29 modes	19x19x5	2600	3.23	9.6
PETROS 3	1.5		20x20x5	3300	3.36	10.7

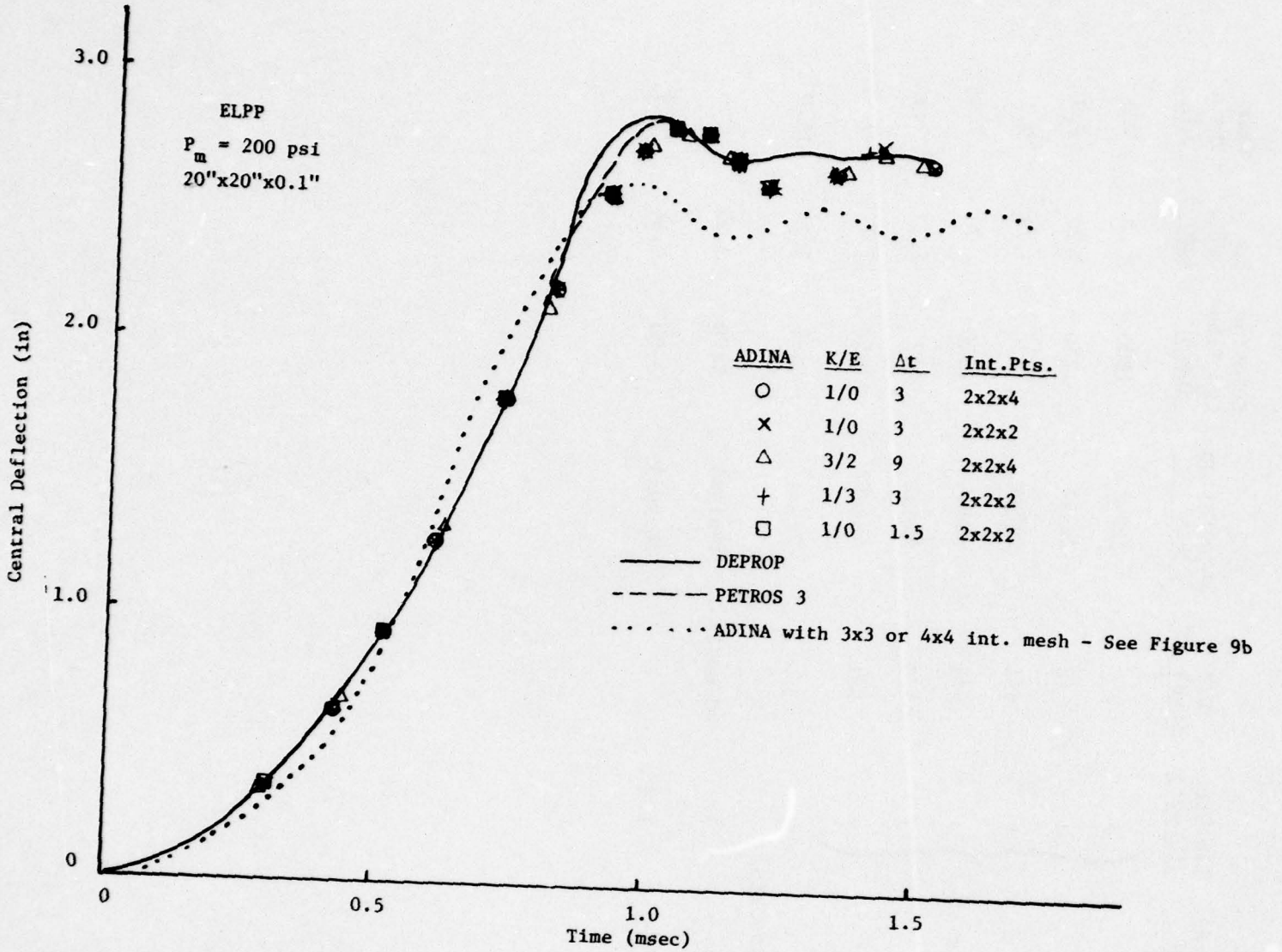

a) Deflection vs time at Plate center. ADINA with 2x2 planar integration mesh vs. DEPROP and PETROS 3 Predictions.

Figure 9. Deformation - time profile for an elastic-perfectly-plastic simply-supported plate.

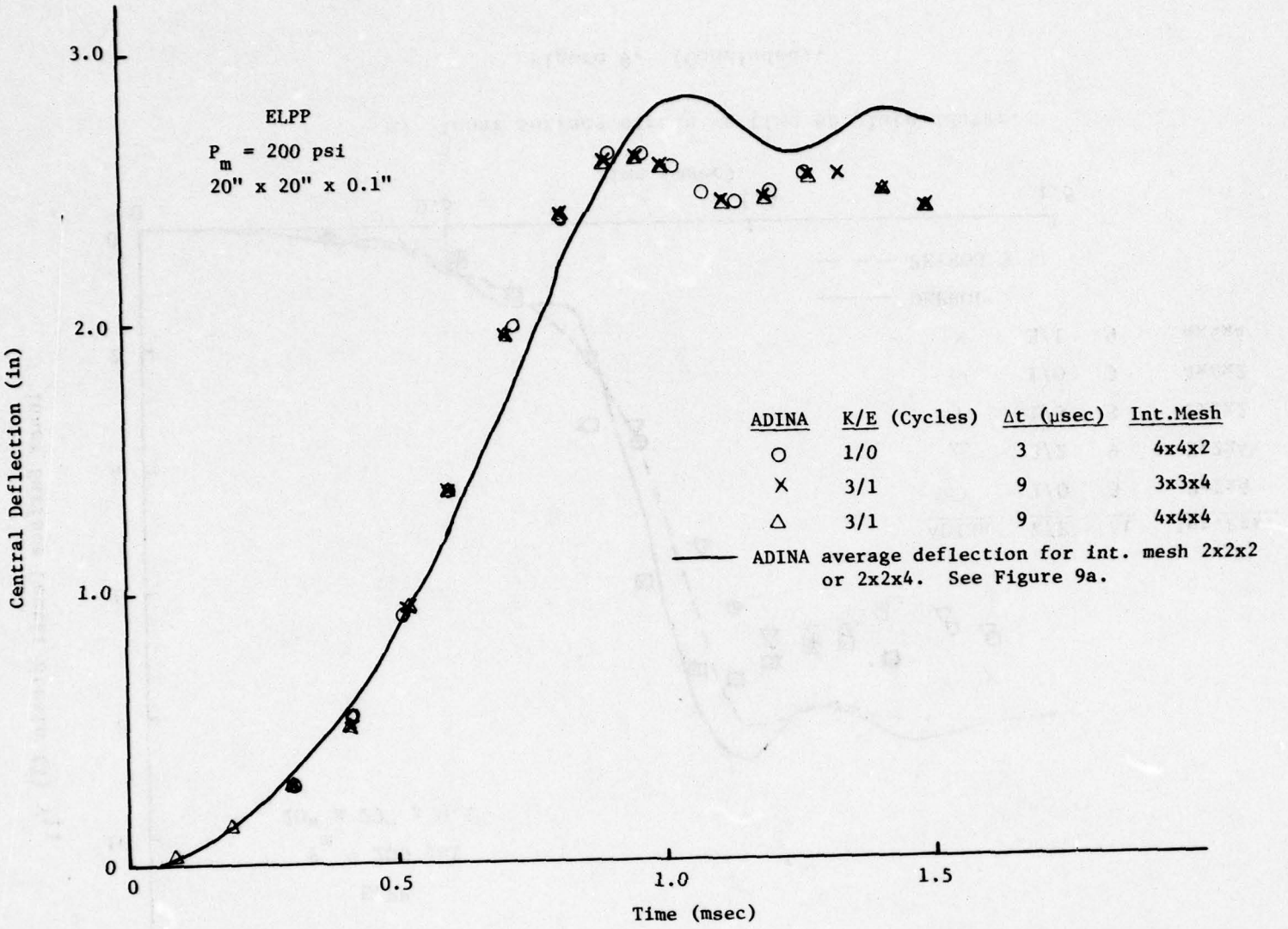

b) Deflection vs time at plate center. ADINA 2x2 vs 3x3 and 4x4 planar integration meshes.

Figure 9. (Continued).

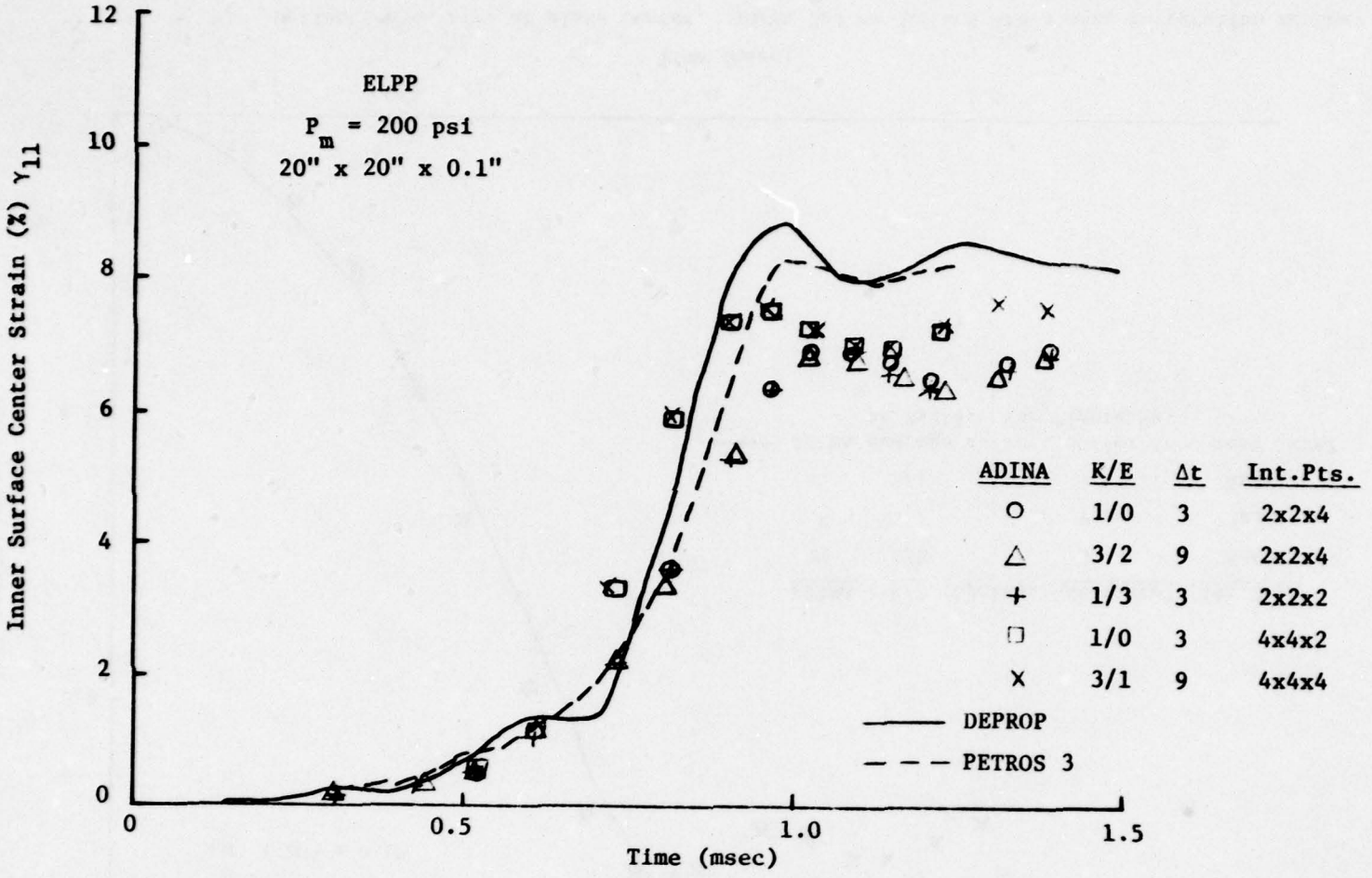

c) Inner surface strain vs time at plate center.

Figure 9. (Concluded).

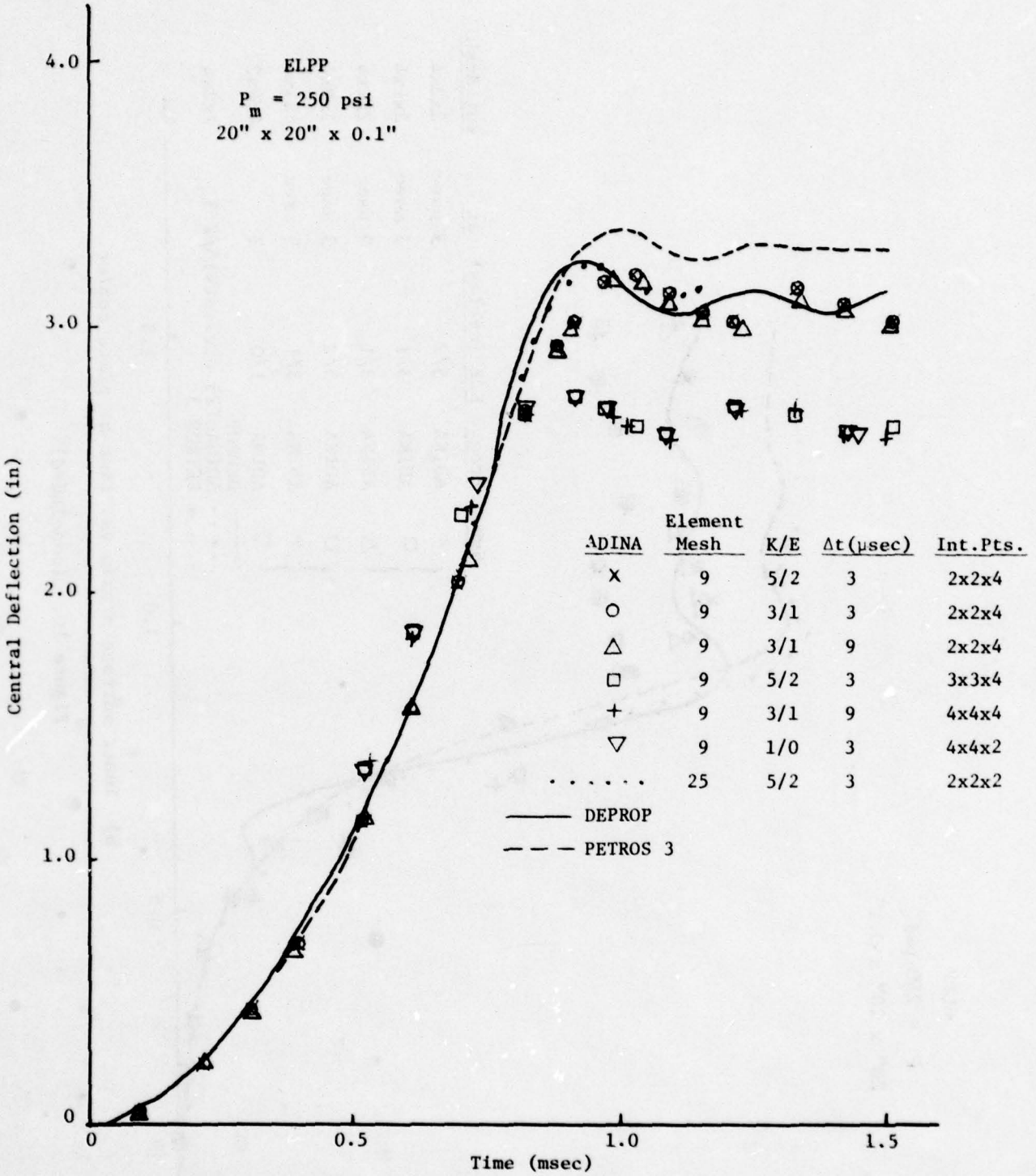

a) Deflection vs. time at plate center.

Figure 10. Deformation - time profile for an elastic-perfectly-plastic clamped plate.

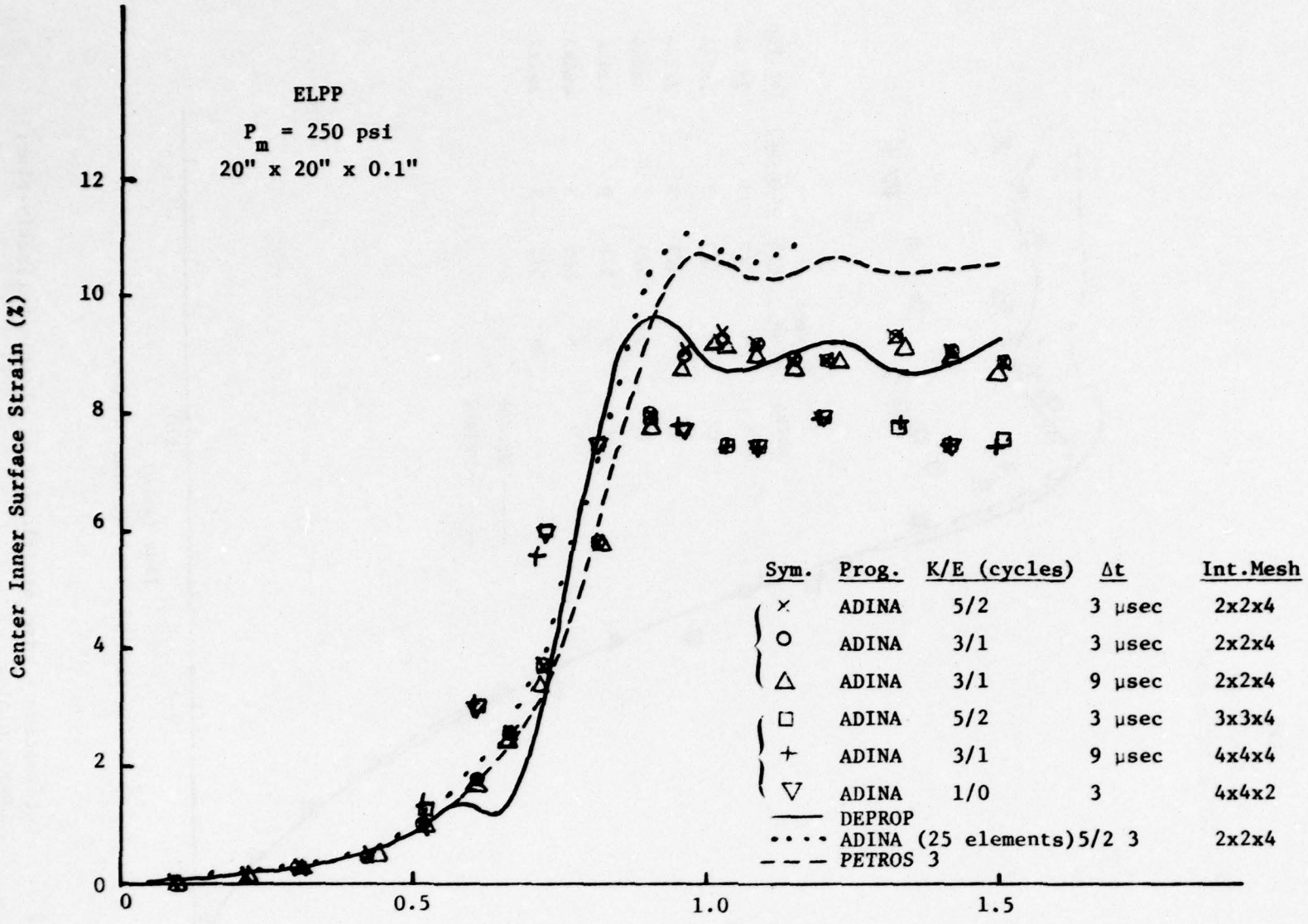

b) Inner surface strain vs. time at plate center.

Figure 10. (concluded).

updating (regardless of the integration grid size or the number of force equilibrium iterations) failed to converge. Alternatively, all the solutions with time steps less than 15 microseconds converged to a solution if periodical stiffness matrix updating was included. For a time step of three microseconds it appears that updating every cycle or every ten cycles converges to the same displacement and strain solution.

Due to the nonlinearity of the deformations and the fact that the ADINA code extrapolates the assumed internal forces at time $t + \Delta t$ from time t for the implicit Newmark operator, it is strongly recommended that force equilibrium iterations be periodically performed. It is seen in Table 4 that for a time step of three microseconds the use of a K/E of 1/3 rather than a K/E of 1/0 requires only a 3.4% increase in solution CPU time. The nature of the implicit operator requires iterations to guarantee a converged solution. This topic will be addressed further in this chapter when the stiffened plate response is discussed.

Solution dependency upon time step size is also analyzed in Tables 4 and 5 and Figures 9 and 10. For the simply supported plate (Table 4 and Figure 9) three variations of time step size were investigated. The time step of three microseconds was selected (as a base value) from the central difference stability time limit for a plate element. Reducing this time step size by fifty percent to 1.5 microseconds resulted in an identical solution with approximately twice the required CPU time (a linear dependency between CPU time and time step size). Increasing the time step size by a factor of three (but attempting to maintain the same time between stiffness updates and equilibrium iterations) resulted in a prediction converging on the same solution value for both displacements and strains. For the simply-supported plate, the time step size was increased by a factor of five and the solutions began to diverge regardless of the fact that the stiffness matrix was updated and equilibrium force iterations were performed every other cycle.

The implicit temporal operators are not unconditionally stable for a nonlinear problem. The case of either the clamped or simply-supported plate subjected to a pressure pulse (two thousand microseconds

in duration, see Figure 8) has a highly nonlinear deformation solution (displacements and strains) which may create a divergent condition for the Newmark operator. Private communications with the ADINA author suggest that for rapidly applied, step input loadings, the Newmark operator can be utilized with a time step no greater than four times the calculated central difference stability limit (see also References 5 and 20). The rapidly applied load tends to excite the discretized mode corresponding to the highest natural frequency of the finite element mesh. Due to the large material and geometric nonlinearities present in the analyzed structure and the wave speeds associated with the deformation propagation, the implicit Newmark operator is time step size limited. (This is also the case with the often used implicit Houbolt operator, References 5 and 20.) An integration scheme is unconditionally stable only if it is assumed that the amplitudes in the modal components which are neglected do not grow, and for nonlinear deformations and impulsive loading all the modes are important.

The greatest variation in solution prediction for either the displacements or the strains occurs when more Gaussian integration stations are used for the in-the-plane directions. Referring back to Subsection 3-3.1, a discussion is presented concerning the "proper" number of integration stations needed for a converged solution. Two Gaussian stations exactly integrate the displacement equation, but three to four Gaussian stations are needed for an exact numerical integration of the strains. Because the three-dimensional continuum element is used for a thin plate, an inappropriately large amount of transverse shear deformation is included in the solution (References 22 and 23), leading to inaccurate displacement estimates if the strains are exactly integrated. It is evident from the tables and figures that a 3 station Gaussian integration provides the same accuracy as a 4 station Gaussian integration, but a two station integration converges to the proper solution value. For the depthwise integration stations, the primary factor constraining the number of stations is the ratio of bending to axial deformation within each element. The depthwise stations are

needed to compute the distribution of stresses. If a membrane is analyzed, then only one station is necessary. For most applications two depthwise stations are sufficient, however, some references (20) imply that, as the amount of elemental bending increases, more depthwise stations are needed, up to four stations. The sample problems presented in this report used two, three, and four depthwise stations and no significant differences in displacement or strain predictions were noticed. However, only central displacements and strains were monitored for this study and the deformations in this region are mainly membrane. If good strain predictions are required in regions of large local bending (i.e. near clamped boundaries) four or more depthwise Gaussian stations may be necessary.

Examining Tables 4 and 5 and Figures 9 and 10 for the unstiffened ELPP plates, the ADINA modeling can be made as accurate and as cost effective as the DEPROP or PETROS 3 solutions. For both the clamped and simply-supported boundary conditions a reasonably good nine element ADINA model can be made with a nine microsecond time step, a K/E of 3/1 or 3/2 and a 2 x 2 x 4 integration mesh. The typical solution time is about 650 CPU seconds on a CDC 6600 for a 1500 microsecond time response. This compares favorably with the twenty-five mode (19 x 19 integration net) DEPROP solution (2600 CPU seconds) or the 20 x 20 finite difference mesh PETROS 3 solution (2870 CPU seconds) for similar levels of displacement predictions.

The possibility exists that the nine element ADINA mesh may be too coarse for clamped plate predictions, especially for predictions near the clamp. The nine element model demonstrated errors of up to 4% in the prediction of the principal strains at a point at which the two strains (x and y) should be identical. A twenty-five element model was tested with a three microsecond time step, a K/E of 5/2 and a 2 x 2 x 4 integration grid for the clamped unstiffened plate. The results are shown in Table 5 and Figure 10. The displacements are essentially the

same as the nine element predictions. However the strain predictions are higher and tend to be closer to the PETROS 3 predictions, whereas all the previous predictions (with the nine elements) converged on the DEPROP prediction.

The DEPROP models used twenty-five combined modes including the seventh symmetric mode. It has been discovered since the publication of Reference 2 that the inclusion of these higher modes with a 15 x 15 integration net might lead to inaccuracies in the strains because the total solution is under integrated. The simply-supported plate uses uniform sinusoidal functions to describe all the mode shapes. However the clamped plate has a complex combination of sinusoidal and hyperbolic functions to represent each mode shape. A minimum of four points may have to be used in each modal loop in order to accurately integrate the entire displacement function. This would require about 50 integration points in each direction on the entire clamped plate to accurately use the seventh mode. When the seventh mode was suppressed and a 19 x 19 integration point net over one-quarter of the plate was used in the DEPROP model, the predictions converged on the PETROS 3 solution.

It is evident for the clamped plate (and possibly for the simply-supported plate) that a nine element mesh in ADINA is adequate for displacements, but a twenty-five element solution predicted the exact same strains in the x and y directions at locations where these strains should be identical due to symmetry; whereas the nine element mesh had about four percent differences for the strain predictions in the two directions. The twenty-five element model could be utilized more economically with a nine microsecond time step and a K/E of 3/2. The CPU time could therefore be reduced from 6500 seconds to about 2900 seconds to be comparable to both the DEPROP and the PETROS 3 solution CPU times.

The preceeding discussion (of correlations for the ADINA prediction of the response of unstiffened, ELPP, clamped or held-simply-supported plates to a uniform linearly decaying blast wave) has established several guidelines for the use of ADINA three-dimensional continuum

elements to model a thin plate. The temporal numerical operator, time step size, cycles for updating the material tangent stiffness matrix, cycles for using force equilibrium iterations, spatial numerical integration point mesh and the element mesh have all been evaluated. Guidelines for the choice of these six modeling variables have been given and the more optimal of these values are used to evaluate the ADINA predictions for an elastic strain hardening material (ELSH), a linear elastic material, and a stiffened elastic perfectly plastic (ELPP) thin plate.

The two material strain hardening models (isotropic and kinematic) available in ADINA have been discussed in Section 3-3.1. Both of these models are used to predict the response of a perfectly clamped unstiffened square thin plate. The plate geometric and material properties are defined in Table 4 and a bilinear stress-strain relation is used to model strain hardening. Table 6 and Figure 11 present the ADINA predictions and their correlation with the DEPROP (bilinear kinematic hardening) and the PETROS 3 (mechanical sublayer model) predictions.

The ADINA predictions with either the isotropic or the kinematic hardening models give the same results for either displacement or strain prediction. The theoretical differences between the two hardening models involve the material response to unloading, loading in the opposite direction (either tension or compression) and then reloading. The "blast-wave" loaded plates examined here are loaded mainly in tension with some unloading but no opposite compression loading and no reloading, allowing the "yield surface" to remain identical for either hardening model. The solution CPU time is essentially the same for either model. The kinematic hardening model compares closely with the empirical data for metals that are cyclically loaded and this hardening model is therefore recommended for general analysis with the ADINA program.

The ADINA predictions correlate well with both the DEPROP and PETROS 3 predictions for displacements; however, as was the case with the ELPP plate, the strain levels are underpredicted. The study with

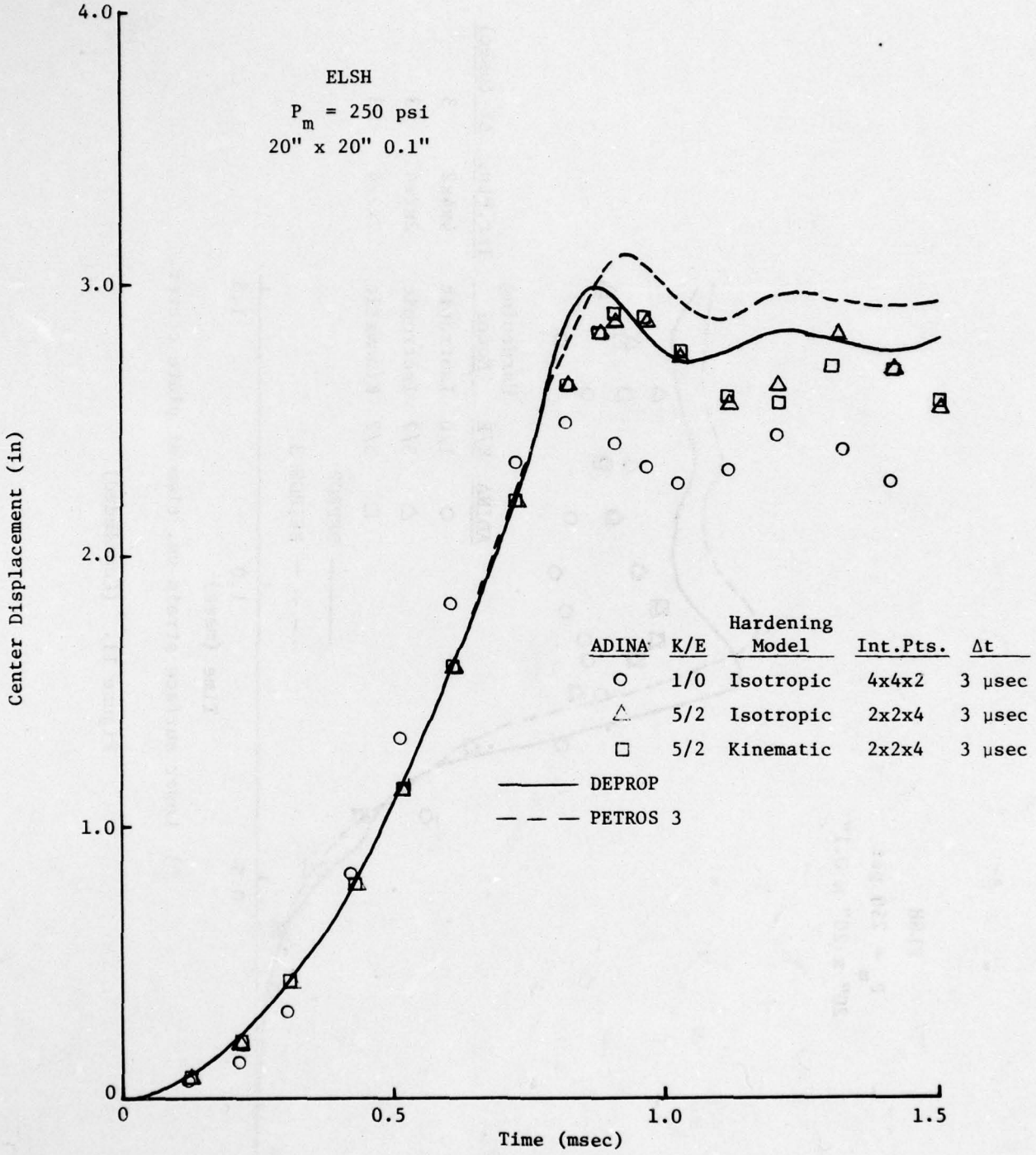

a) Deflection vs. time at plate center.

Figure 11. Deformation - time profile for an elastic-strain hardening clamped plate.

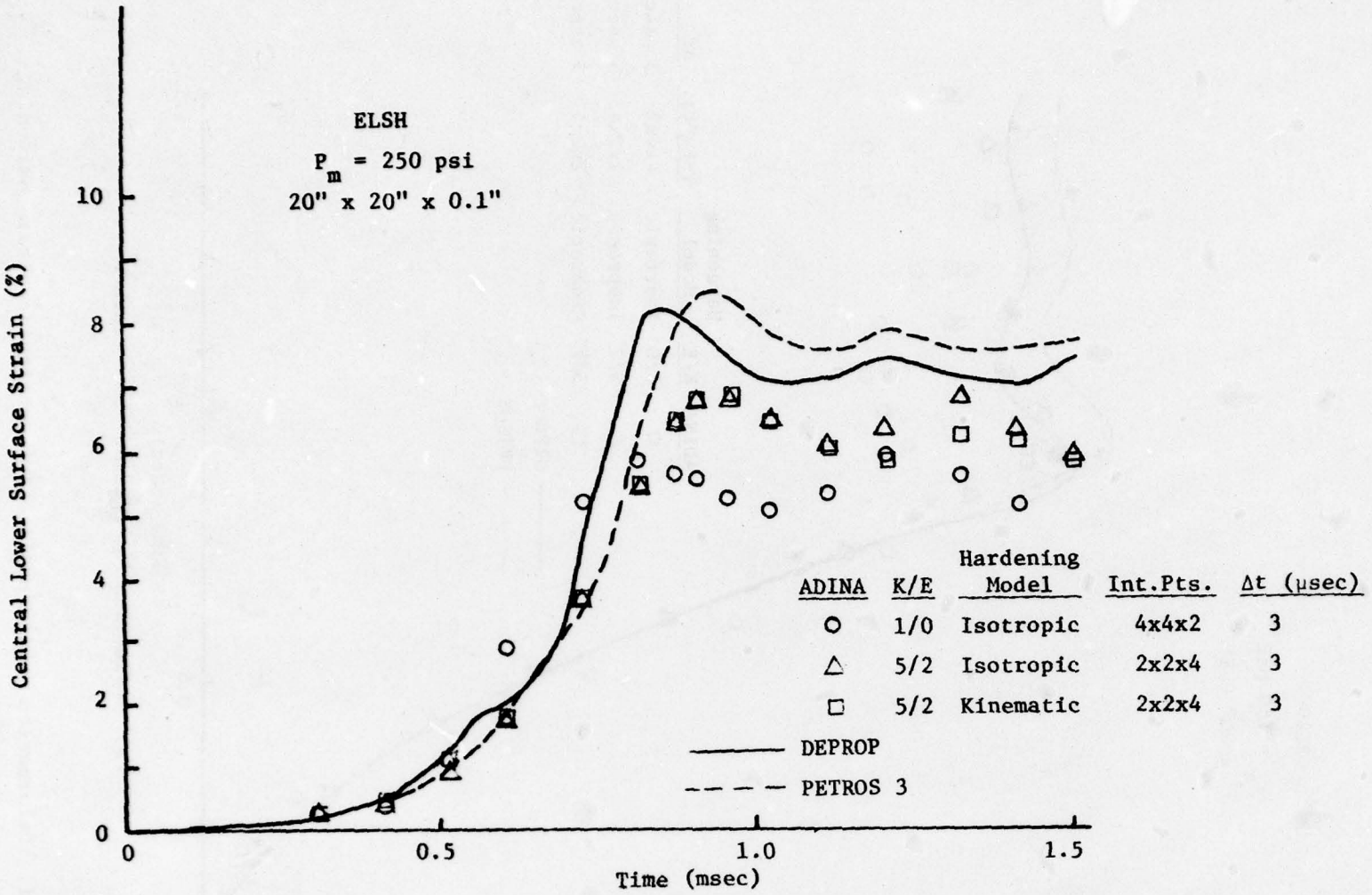

b) Lower surface strain vs. time at plate center.

Figure 11. (Concluded).

the ELPP unstiffened plates demonstrated that the nine element mesh may be too crude to obtain converged strain predictions and that a twenty-five element mesh may be more appropriate.

The ADINA predictions for an elastic plate undergoing large displacement response are now examined. An unstiffened clamped plate, Table 4, subjected to a uniform, timewise linearly decaying pressure pulse, Figure 8, with a maximum initial pressure, P_m, of 100 psi, is analyzed and compared with DEPROP and PETROS 3 predictions.

It is evident from Table 7 that the choice of numerical integration grid size is important for the elastic response predictions as well as for the previously analyzed plastic response predictions. The peak deflections tend to be underpredicted (similar to Tables 4, 5 and 6) for the 4 x 4 planar integration point grid. Table 7 and Figure 12a show that the displacement predictions with the 2 x 2 integration point grid have nearly the same amplitude and phasing as the DEPROP and PETROS 3 predictions. It should be noted that the ADINA strain predictions (Figure 12b) for the two different integration point grids are nearly identical in amplitude, slightly different in peak strain phasing but apparently in phase for long time strain response.

It is appropriate to point out that the strain predictions for the ADINA program are not exactly at the center of the plate nor are they exactly at the inner surface. The ADINA strain locations are identical to the Gaussian station locations and therefore vary as the integration grid changes. For the large nonlinear plastic deformation encountered in the previous models examined in this study this was a small problem because the strain at or near the plate center was of similiar magnitude and there was little bending compared to stretching at the plate center (approximately 96% membrane strain and 4% bending strain). However, for the elastic plate response, the strain gradients are comparatively large at the plate center and bending is the primary deformation mode present; therefore, the ADINA strain predictions are expected to be lower than the corresponding DEPROP and PETROS 3 predictions which are located at the exact inner surface of the plate

Table 7. Numerical predictions for a clamped, unstiffened, elastic plate subjected to a uniform, linearly decaying blast wave load.[+]

Numerical Method	Formulation	Timestep Size Δt (sec)	K/E Cycles	Integration Point Grid	Solution CPU Time (sec)	Peak Defl. (in)	Peak Strain (%)
ADINA	Total Lagrangian	3	1/0	4x4x2	4345	1.08	0.91
		9	3/1	4x4x2	975	1.08	0.91
		9	3/1	2x2x4	545	1.19	0.95
		9	3/1	2x2x2	335	1.19	0.87
		9	0/1	2x2x2	190	1.14	0.80
	Updated Lagrangian	9	3/1	2x2x2	390	1.20	0.85
		9	0/1	2x2x2	140	1.15	0.78
DEPROP	Total Lagrangian	3.0	25 modes	15x15x1	855	1.24	1.15
PETROS 3	Total Lagrangian	1.5		20x20x2	1600	1.25	1.24

[+] P_m is equal to 100 psi for elastic response; see Figure 8.

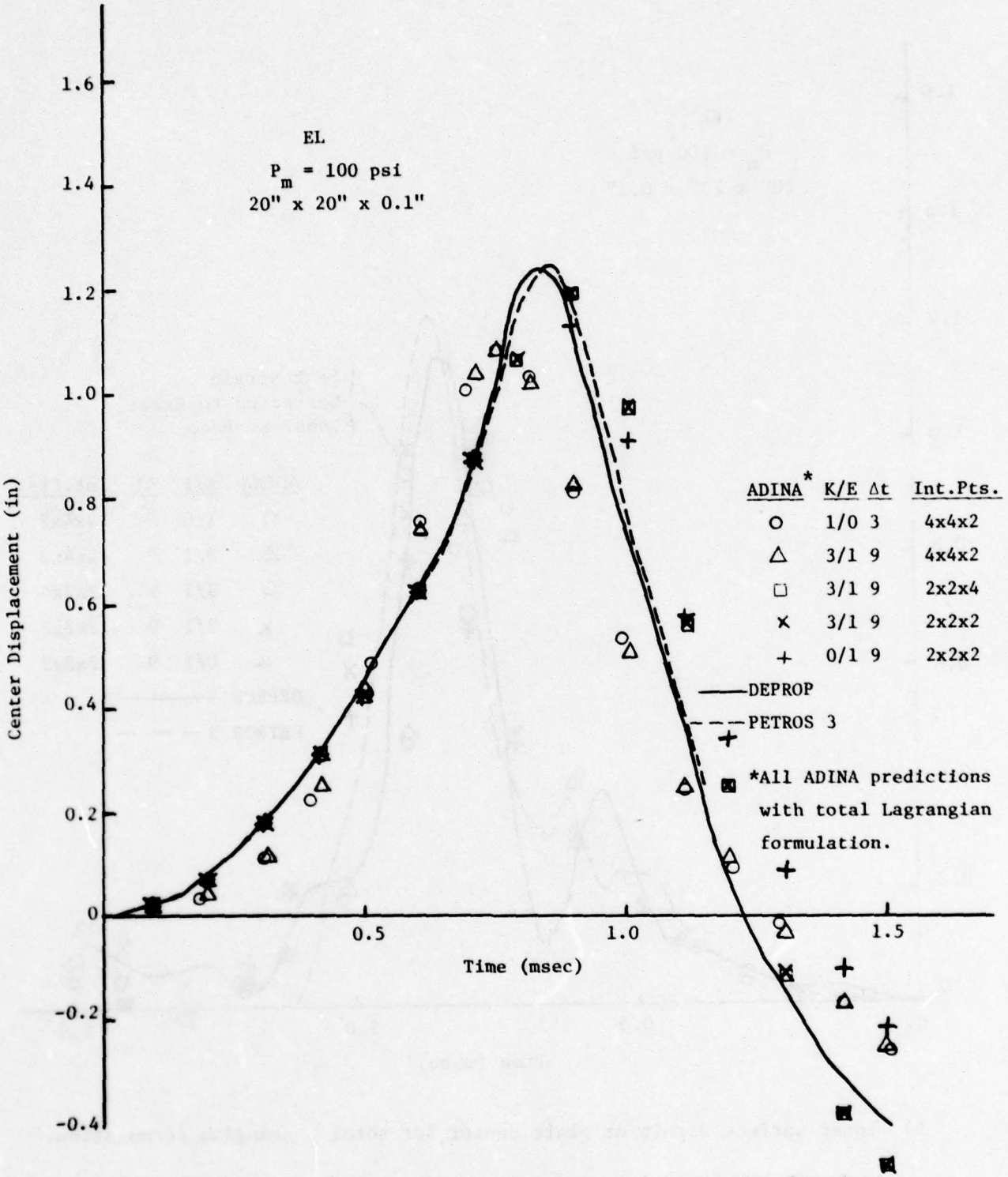

a) Deflection vs. time at plate center for total Lagrangian formulation.

Figure 12. Deformation - time profile for an elastic clamped plate.

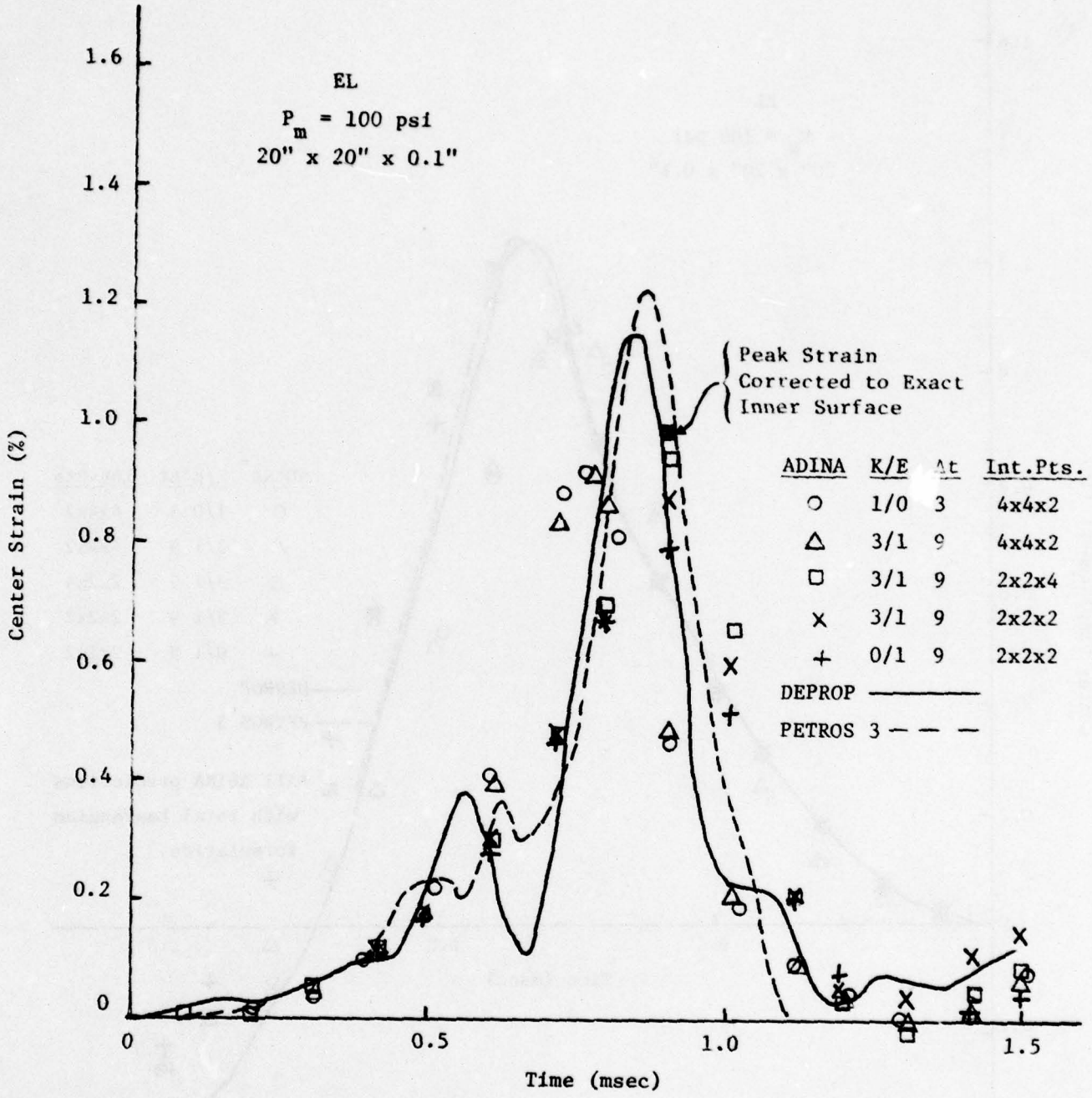

b) Inner surface strain at plate center for total Lagrangian formulation.

Figure 12. (Continued).

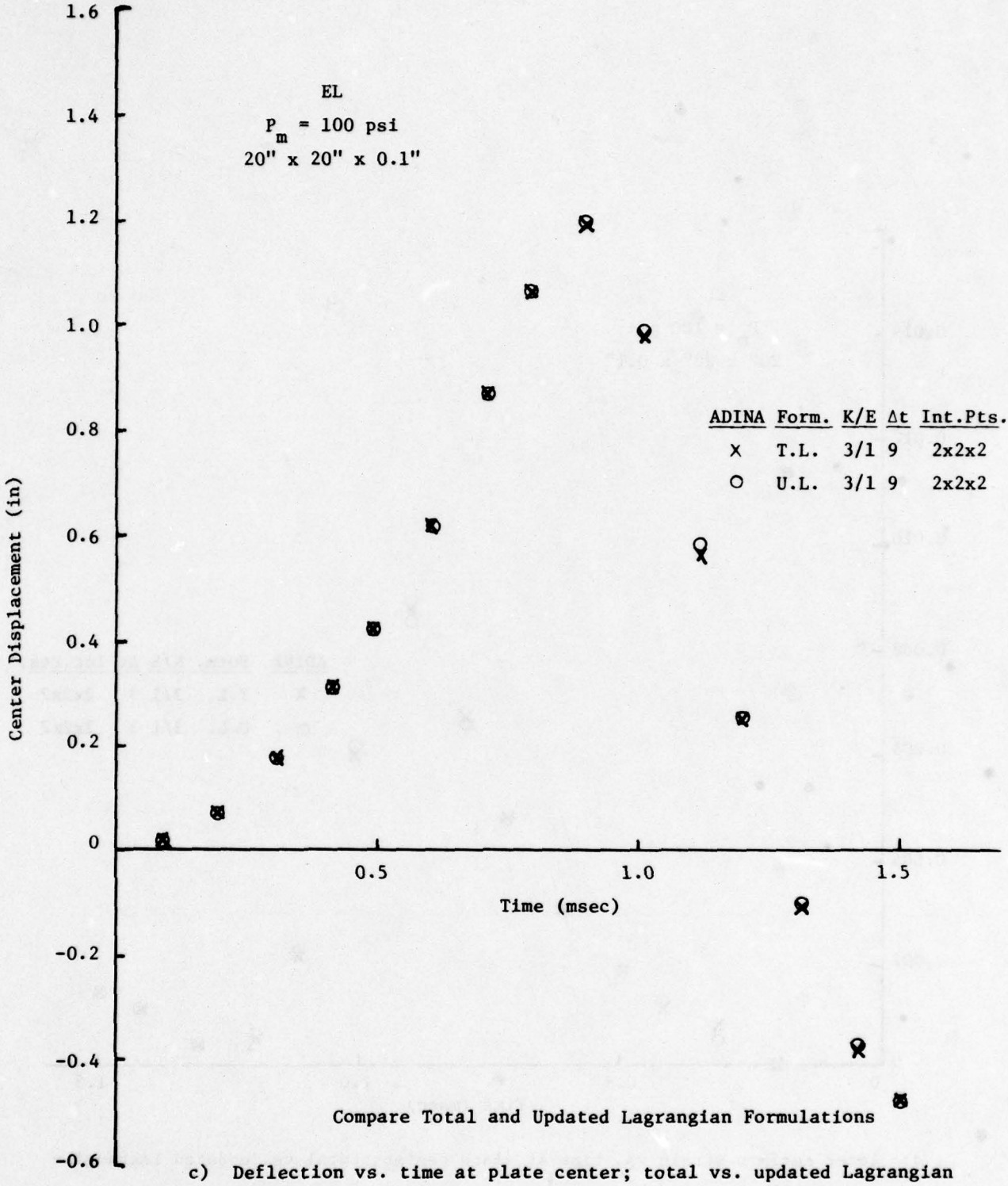

c) Deflection vs. time at plate center; total vs. updated Lagrangian formulations.

Figure 12. (Continued).

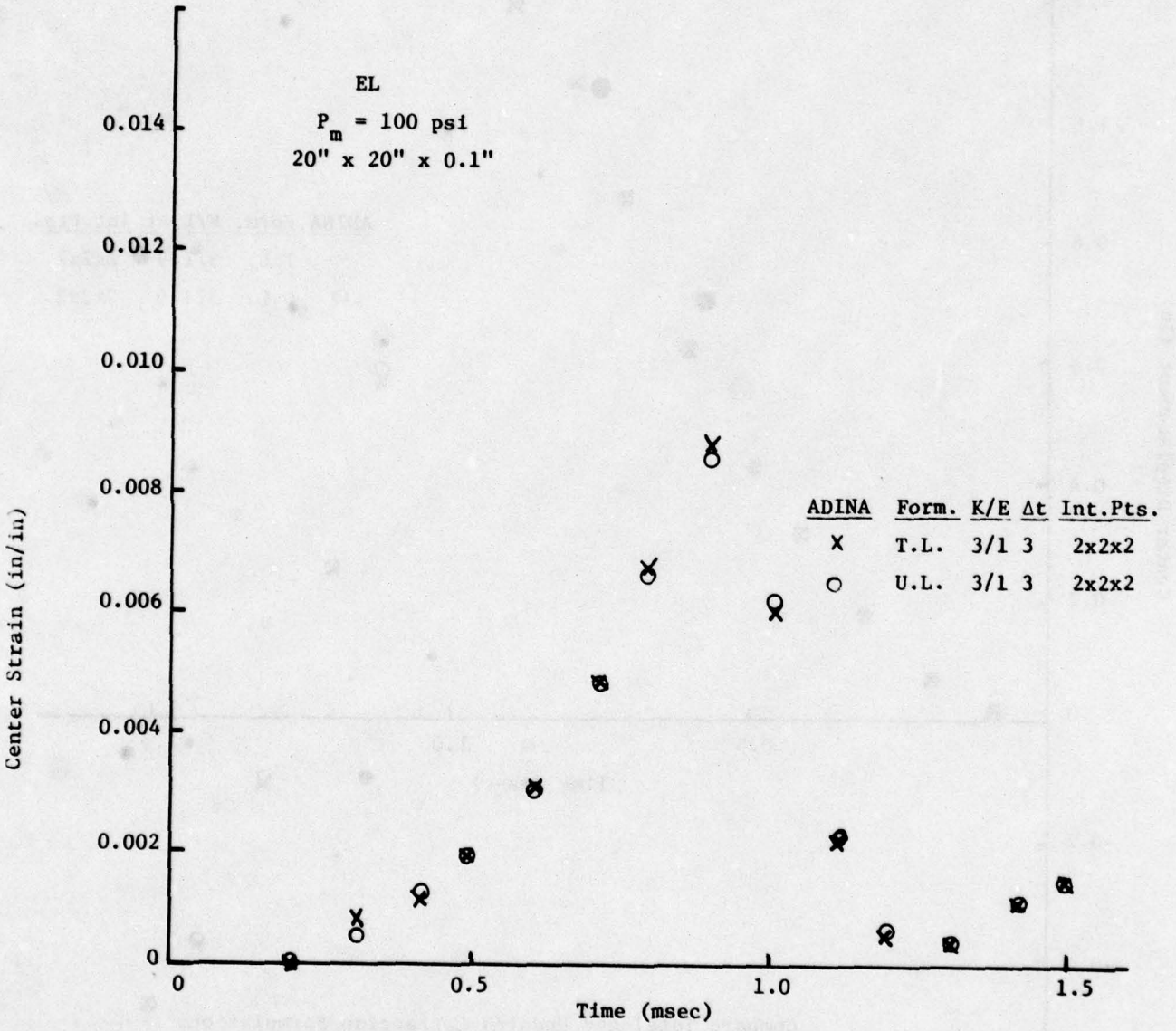

d) Inner surface strain vs. time at plate center, total vs. updated Lagrangian formulations.

Figure 12. (Continued).

center. For the ADINA 4 x 4 grid, the strain prediction location is 0.327 in. from the plate center or 2.3% of the total plate diagonal from the center, and for the 2 x 2 grid, the strain location is 0.996 in. from the plate center or 7.0% of the total plate diagonal from the center. (This strain location information is the same for all of the ADINA predictions presented in this study, see Figure 13.) Figure 12b shows "corrected" peak strain predictions for two ADINA models differing only in the number of depthwise Gaussian stations. It is noted from Figure 12b that the peak strain predictions are now identical for the two models. The ADINA isoparametric 3-D element follows a linear variation through the thickness and this was applied to the original strain prediction to obtain the predicted strain at the inner surface.

This examination of the elastic plate indicates that the integration grid size is a universal problem for a three dimensional element used to model a thin plate structure, and indicates also the problems that could be encountered with ADINA in determining maximum strains if the strain information can not be obtained easily at the plate center.

The elastic plate is modeled with a total Lagrangian formulation and a linear isotropic material model. For the three-dimensional continuum ADINA element the updated Lagrangian formulation can not be used except with the linear isotropic material model. Therefore, one model with the updated Lagrangian formulation was generated and Figures 12c and 12d and Table 7 show that the predictions are identical with those obtained with a total Lagrangian formulation and the CPU time is slightly greater for the updated Lagrangian formulation model. An additional total Lagrangian model was tested with no updates of the tangent stiffness matrix. Figures 12a and 12b show that some periodical stiffness matrix updating is needed, even for linear elastic bending problems. This is the one major drawback with the use of an implicit Newmark operator with a conventional formulation compared with an explicit central difference operator with an unconventional formulation. However the central difference operator can not be used with a 3-D element approximation of a thin plate as mentioned earlier in Section 3-3.1

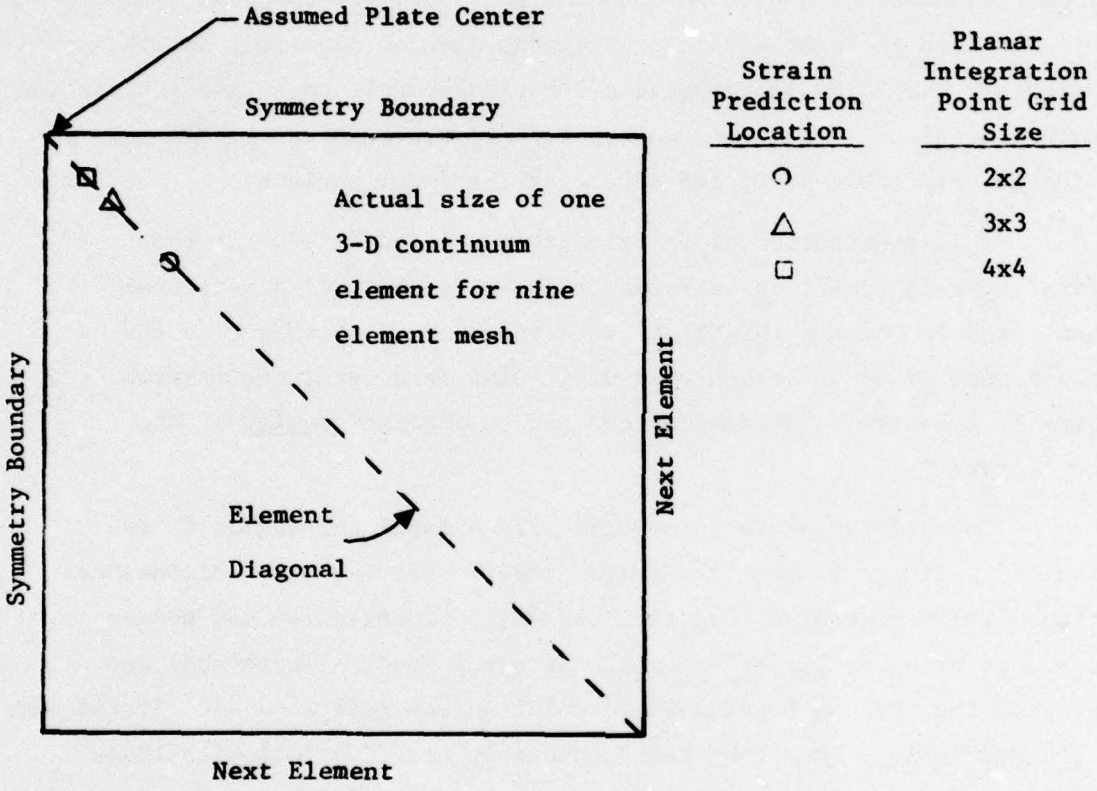

Figure 13. ADINA strain prediction locations for the nine element mesh.

The ELPP analysis is applied to the stiffened plate model and the predictions are shown in Table 8 and Figure 14 for both the simply-supported and clamped boundary conditions. Preliminary predictions for both configurations used the 3 x 3 or 4 x 4 in-plane Gaussian station grid, and both Table 8 and Figure 14a show that these predictions are divergent from the expected displacement solution, as given by the DEPROP prediction. This situation was discussed earlier in this report for the unstiffend plate configurations and is merely presented here for confirmation. It should be noted that the displacements are predicted poorly but that the strain levels are consistent for either the 2 x 2 or the 4 x 4 in-plane Gaussian station grid. This is the expected result because the strain equations are integrated exactly, but an artifically large tranverse strain is introduced into the system and causes the displacements to be incorrectly predicted. The displacements predicted by either a 3 x 3 or a 4 x 4 planar grid are identical and only the 2 x 2 planar integration point grid predicts displacement levels that are consistent with the DEPROP prediction. Because the stiffener in the ADINA model is not properly offset from the plate, it is expected that the displacements from the DEPROP prediction will be lower than the ADINA prediction.

An "economically restrictive" time solution was used for both the clamped and simply supported stiffened plates. The model consists of a three microsecond time step and a K/E of 3/1, producing a solution time of between 2000 and 2200 CPU seconds. (It is interesting to note that the solution time, for identical timewise models of clamped or simply-supported plates, tends to be greater for the simply-supported configuration. This is due to the greater number of degrees of freedom included in the global simply-supported plate model compared with the global clamped plate model.) This "restrictive" modeling is used to insure that the coupled response of the beam stiffener and the plate elements is analyzed correctly and that a convergent solution is obtained. It can be seen in Table 8 that (for both boundary condition configurations) the overall solution time is comparable to the CPU solution time for the DEPROP analysis. (The CPU times are similar between ADINA and DEPROP

Table 8. Numerical predictions for a stiffened, elastic perfectly plastic plate subjected to a uniform, linearly decaying blast wave load.[+]

Numerical Method	Boundary Condition	Timestep Size (Δt) (sec)	K/E Cycles	Integration Point Grid	Solution CPU Time Sec	Peak Defl. (in)	Peak[*] Strain x/y (%)
ADINA	Held-simply-supported	3	1/0	4x4x2	Diverged		
ADINA	Held-simply-supported	3	3/1	2x2x4	2220	2.48	5.16/5.42
DEPROP	Held-simply-supported	3	30 modes	19x19x5	3085	2.20	2.43/5.62
ADINA	Clamped	3	1/0	4x4x2	5545	2.64	8.3/7.1
ADINA	Clamped	3	3/1	3x3x4	3855	2.62	7.7/6.6
ADINA	Clamped	3	3/1	2x2x4	2000	3.07	7.5/8.2
DEPROP	Clamped	2	30 modes	19x19x5	4675	2.78	4.0/5.1

[+] P_m for clamped plate is 350 psi; P_m for held-simply-supported plate is 250 psi.

[*] Peak strain at plate center; x direction normal to stiffener; y direction parallel to stiffener.

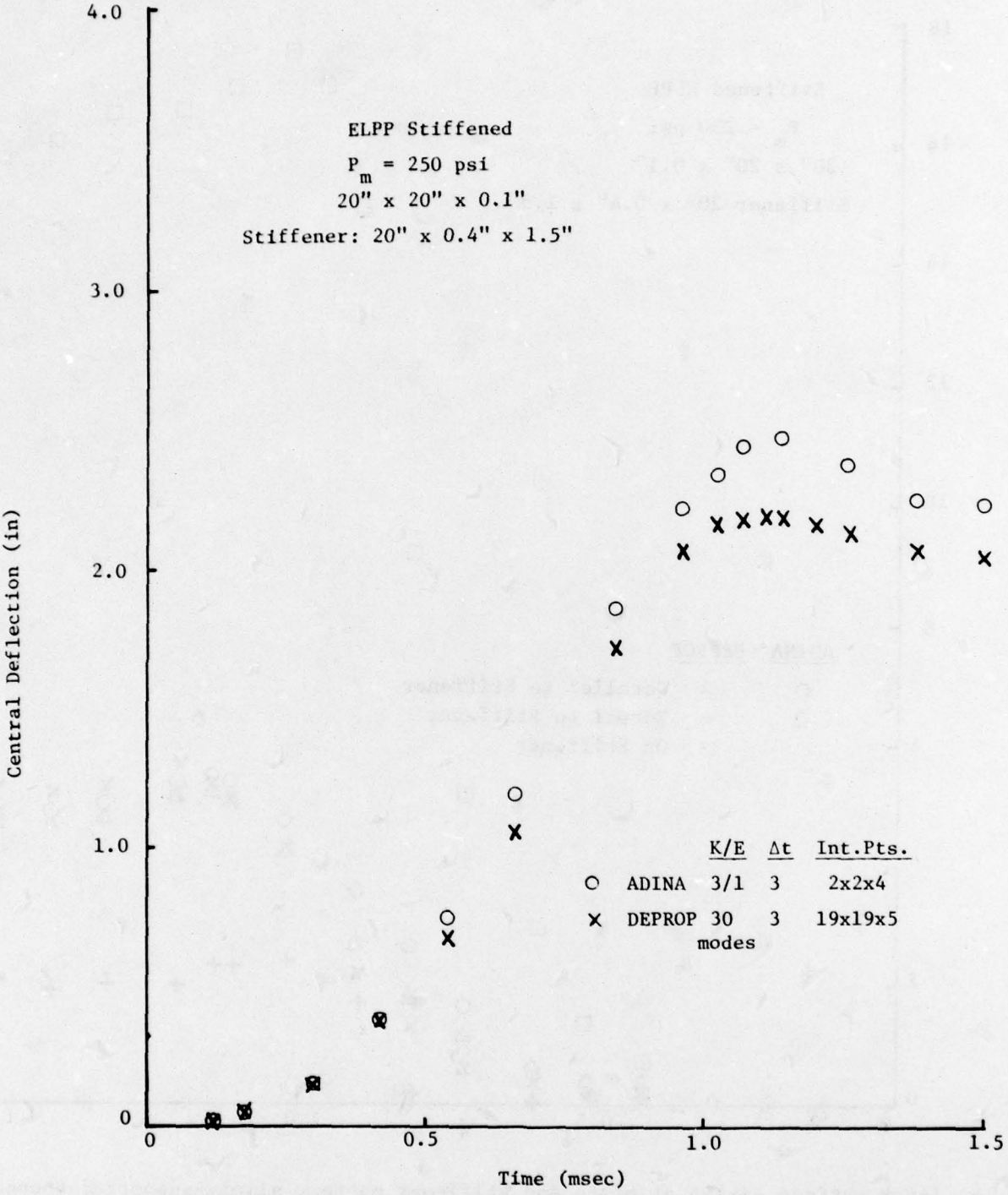

a) Deflection vs. time at plate center; simply-supported boundaries.

Figure 14. Deformation - Time profiles for an elastic-perfectly-plastic stiffened, clamped or simply-supported plate.

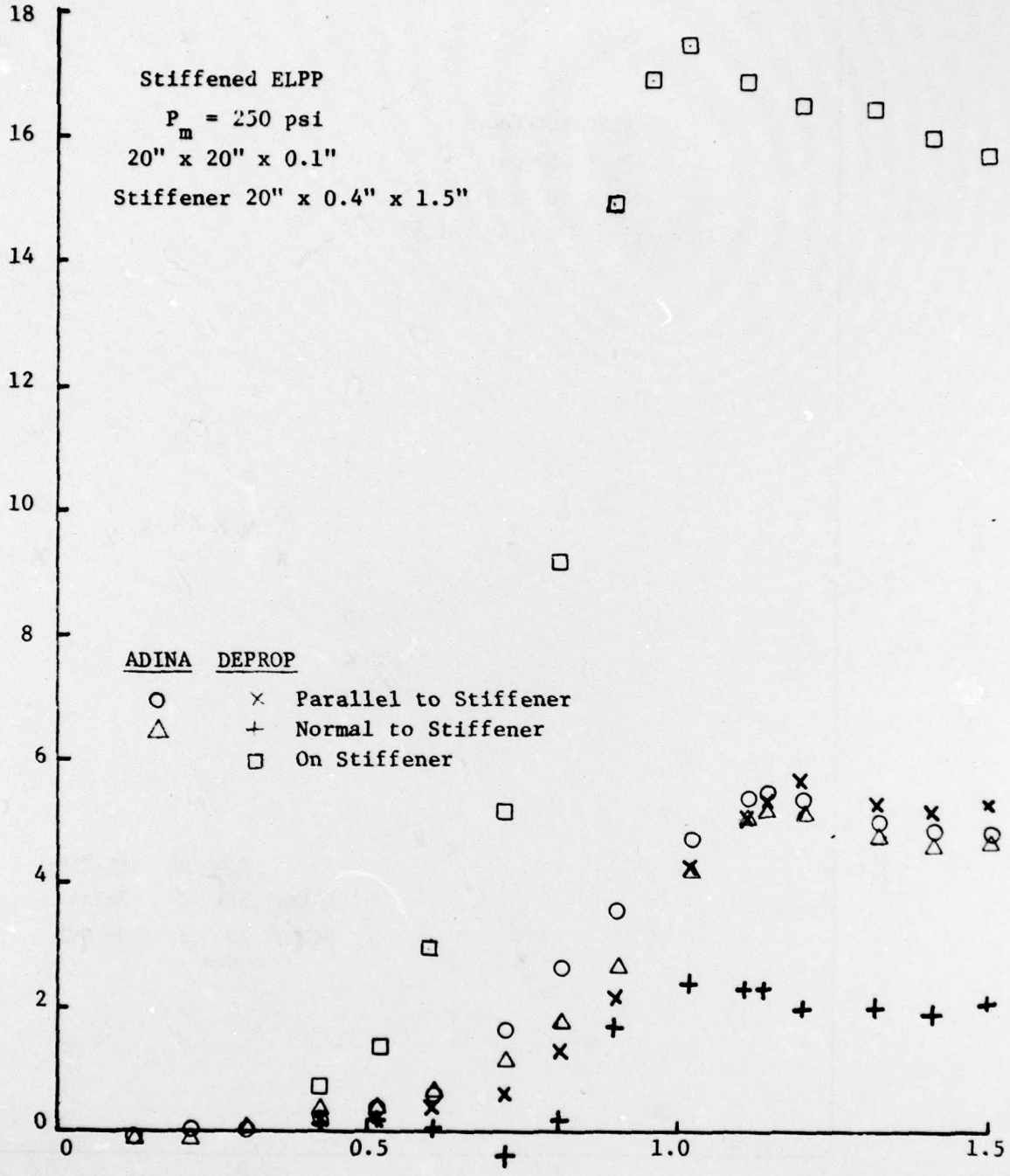

b) Inner surface strain at plate and stiffener center; simply-supported boundaries.

Figure 14. (Continued).

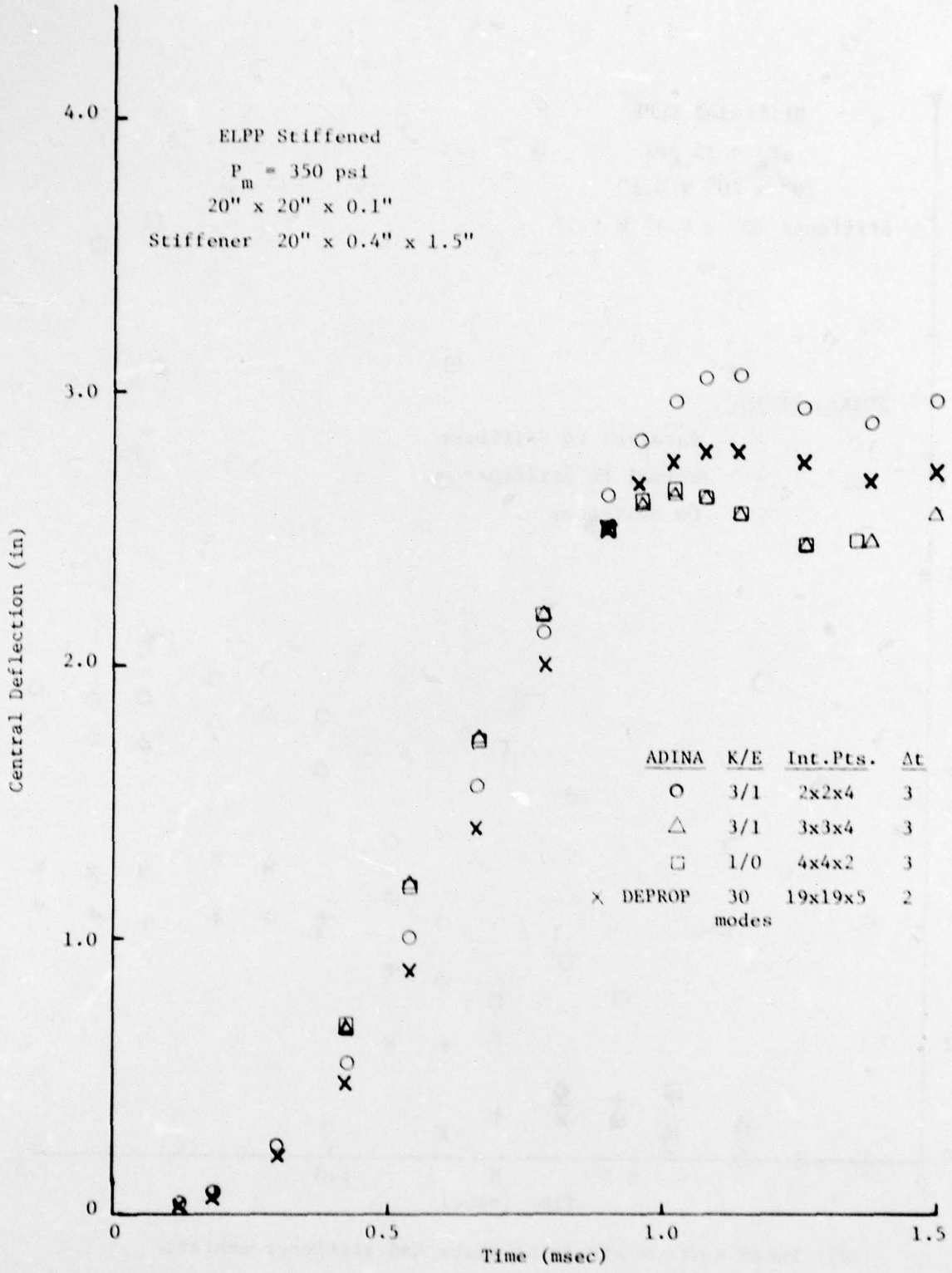

c) Deflection vs. time at plate center; clamped boundaries.

Figure 14. (Continued).

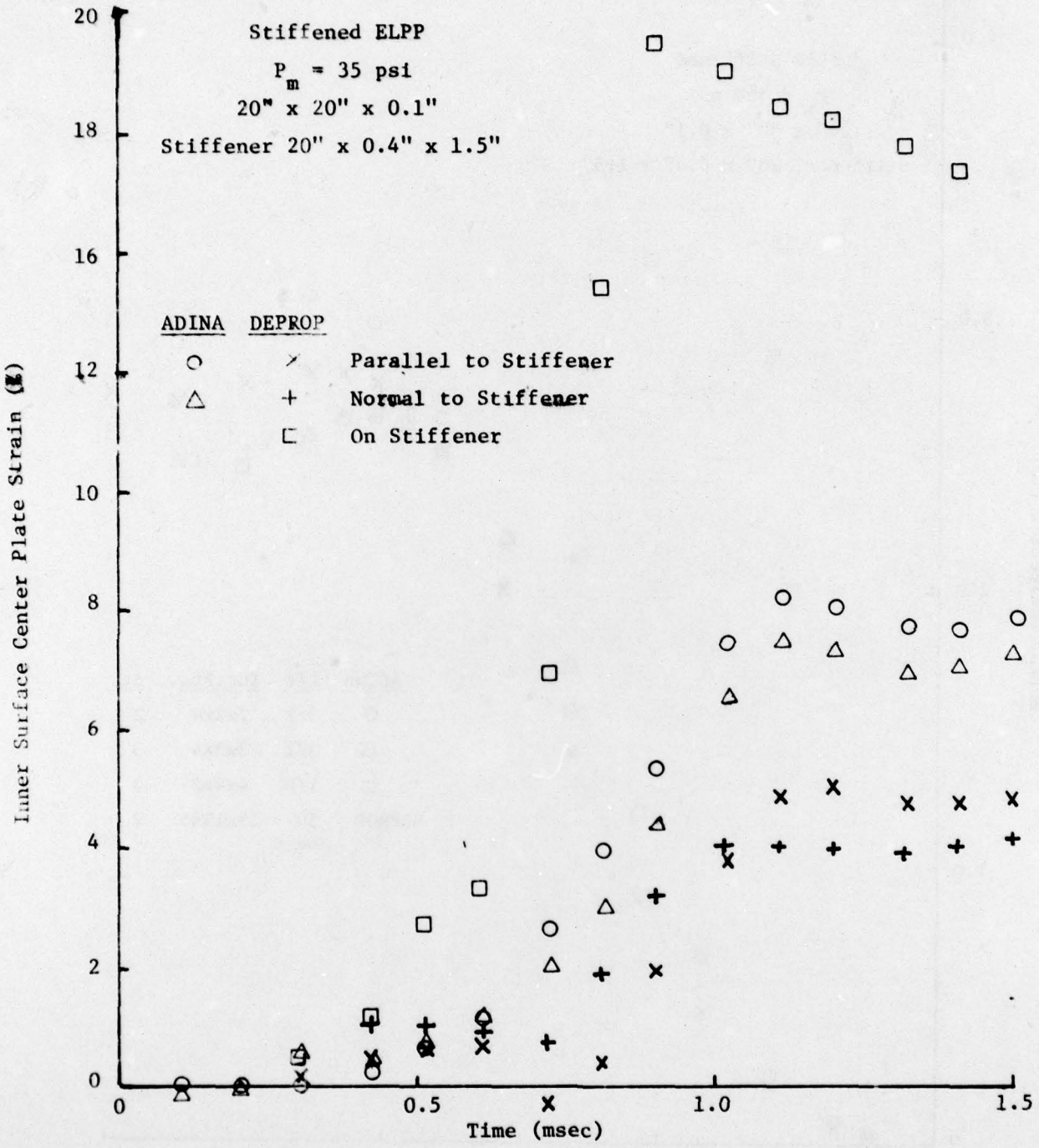

d) Inner surface strain at plate and stiffener center; clamped boundaries.

Figure 14. (Concluded).

if the ADINA times are modified to include a slightly larger time step and a twenty-five element mesh for strain prediction accuracy.)

3-4 SUMMARY OF ADINA STRUCTURAL RESPONSE PREDICTIONS.

At present the ADINA code contains a 3-D beam element and a 3-D isoparametric continuum element both of which can be used in modeling nonlinear structures. The elements have both total and updated Lagrangian formulations and the Newmark and central difference temporal operators available. However, the beam element is restricted to use the updated Lagrangian formulation and the nonlinear continuum element can only use the total Lagrangian formulation.

The central difference temporal operator appears to be the most economical to use with the beam element for large step-load functions, typical of blast wave overpressure loading, but can not be used with the continuum element to model a thin plate. The continuum element with the Newmark operator must have periodical updating of the stiffness matrix and should have periodical force equilibrium iterations to insure a converged solution. Within a reasonable limit, the choice of the time between updates and iterations has a small influence on accuracy but a major influence on solution cost based on computer CPU time. (It should be noted that the central difference operator requires neither updating nor equilibrium iterations.) Another factor having a major influence upon the solution CPU time is the choice of the time step size. The central difference operator is restricted by a stability time limit and the Newmark operator can be utilized with a maximum time step size only four times greater than the central difference stability limit if a large step-loading function is being analyzed.

The major factors influencing the solution accuracy appear to be the integration grid size and the size of the finite element mesh. For the plate model it appears that the nine element mesh was satisfactory for displacement predictions but that a twenty-five element mesh is necessary for a converged strain prediction, especially for the clamped plate. No similiar deductions could be made for the beam elements because strain predictions were not available and displacement predictions are not as sensitive to mesh size.

Within each element the size of the integration point mesh was an important influence on the predictive accuracy. For both the beam and the continuum element a spatial formulation using under integration is necessary for an accurate displacement prediction. The beam element uses the closed Newton-Cotes spatial integration formulation which has an oscillatory convergence as the number of integration points is increased. It was found that five integration points along the element length and three integration points through the element thickness represent the best choice for the nonlinear beam analyses that were examined. The continuum element uses a Gaussian spatial integration formulation; however, the three-dimensionality of the element introduces artifically large transverse shear strains if the strains are fully integrated for an element length to thickness ratio much greater than one. A 2 x 2 planar Gaussian station grid completely integrates the displacements but underintegrates the strains and in so doing obtains a better overall response prediction. This situation for both the beam and the continuum element is theoretically unsatisfactory. The spatial integration on the beam element could be improved if an alternate integration formulation were used. Either an iterative low-order Newton-Cotes formulation or a Gaussian formulation would guarantee improved accuracy as the number of stations is increased on the beam element. The situation for the continuum element is one that has been identified for many years in the finite element field and can only be improved by using more continuum elements and underintegrating within each one or by utilizing a thin plate or shell nonlinear element. The ADINA code will soon have a nonlinear thin shell element which should improve the solution accuracy. However this element will have to be studied for its applicability to blast wave overpressure loading on thin shell structures.

The continuum element was examined for several unstiffened plate modelings. Two different boundary conditions were examined, the perfectly clamped boundary and the held-simply-supported boundary. No major difficulty was experienced in using either boundary condition and the solution CPU time for the held-simply-supported boundary was slightly larger than the clamped boundary plate which is consistent with the fact

that there are more global degrees of freedom in the held-simply-supported plate model. The continuum element possesses only translational degrees of freedom. Modeling a simply-supported edge with the continuum element requires an artificial combination of upper and lower surface degree of freedom constraints. This boundary definition apparently works adequately to model plate-like structures that are not rigidly fixed at the edges.

The continuum element was examined for three different material modelings: perfectly elastic (EL), elastic-perfectly-plastic (ELPP) and elastic-strain hardening (ELSH). Predictions with all three modelings compared favorably with corresponding DEPROP and PETROS 3 predictions when the appropriate integration grid and element mesh size were chosen. (The modeling required a 2 x 2 x 4 integration grid and a nine element mesh for displacement prediction accuracy or a twenty-five element mesh for strain prediction accuracy.) For all three material models using the Newmark temporal integration operator both updating of the stiffness matrix and an equilibrium force iteration were required to guarantee a converged solution. The ELSH modeling was not utilized with a cyclical loading and therefore both the isotropic and the kinematic strain hardening models in the ADINA code gave similiar predictions for both displacements and strains and used identical amounts of computer CPU time. Both the DEPROP and the PETROS 3 codes use either a kinematic or a mechanical sublayer strain hardening model and it is recommended that ADINA be used with the kinematic model for nonlinear metal material deformations.

The continuum element was combined with the beam element to provide a model for a stiffened plate. Little difficulty was encountered in establishing this combined element model and the predictions were similiar to the DEPROP prediction (PETROS 3 can not accommodate stiffeners). However the ADINA code does not presently allow a beam element to be attached to a plate node with an offset. Therefore the neutral axis of the beam is coexistent with the plate surface to which the beam element is attached. This does not allow an accurate model of a stiffened plate to be assembled, and the resultant stiffened plate mass distribution and bending stiffness will be inaccurately modeled.

Strain printouts from the ADINA program are inadequate for general engineering utilization. The as-received ADINA code does not provide strain information but instead prints stresses at user designated integration station locations. Stress information is ambiguous and misleading for nonlinear plastic deformation analysis. Strain printout for the continuum element was added to the ADINA code; however, it has not yet been properly added for the beam element strains. For the nonlinear continuum element, strain printouts are available only at integration station locations. This is inadequate most of the time because strain information is needed at the nodal locations and along the inner and outer surfaces. This information could be obtained with some extensive revisions of the ADINA code. An updated version of the ADINA code is expected shortly but it is unknown whether the needed strain information will be provided.

The overall examination of the ADINA code shows that for simple structural geometries (beam or plate) displacement and some strain predictions comparable to DEPROB, DEPROP and PETROS 3 predictions can be obtained for the same approximate CPU solution time on a CDC 6600 computer. The ADINA code, in its present configuration, can not properly model all the beam and plate configurations that are readily identifiable with aircraft-type structures. However, the ADINA program with some revisions could be made into an adequate structural analysis program for blast wave overpressure effects on aircraft structures.

SECTION 4
CONCLUSIONS AND RECOMMENDATIONS

The ADINA finite element program was evaluated to determine whether the program could be an applicable structural response routine for the NOVA aircraft overpressure vulnerability code. The evaluation concentrated on the accuracy and computational efficiency of transient response solutions of beams, unstiffened panels and stiffened panels. The response of a more complex aircraft structure should also be evaluated after the final version of ADINA is issued shortly and the thin shell element is available. However, based on the present evaluation of the current ADINA program the following general conclusions are given:

1) ADINA is a well organized and documented code which will accommodate possible future modifications and extensions to satisfy the needs of an aircraft overpressure vulnerability code.

2) ADINA is theoretically and numerically sound and provides the full nonlinear capability, both geometrically and physically, that is required for damage levels considered in aircraft vulnerability analyses.

3) The final version of ADINA will provide a sophisticated finite element library of all the basic types of elements needed to model idealized structures, but lacks the variations in these basic elements, such as multilayered skin and various shaped stringers and frame cross sections, that are required to model many actual aircraft structures.

4) The results from the response comparisons between ADINA and other nonlinear structural codes for simple structures indicate that the accuracy and computational efficiency in the ADINA finite element code are comparable to those of the DEPROB, DEPROP and PETROS codes which are based on discretization methods other than the finite element method.

5) ADINA is a proprietary code with a definite restriction on the distribution of the source deck of the code outside the ADINA Users' Group. If ADINA were incorporated into the NOVA vulnerability code, the limits on the distribution of the new NOVA code is presently uncertain.

In the event that future sophistication of the structural response analysis of the NOVA aircraft overpressure vulnerability code is warranted, the following recommendations are presented for future work with the ADINA code:

1) The efficiency of the new thin shell element should be evaluated for one of the simple plate models used in Section 3. Then the thin shell and beam elements should be used to model a more complex structure representative of a stiffened aircraft substructure and the transient response evaluated relative to that obtained using the stiffened panel version of DEPROP in NOVA-2S.

2) The capability of the beam element in ADINA should be extended to include cross sectional shapes found in aircraft structures, such as I-sections, Z-sections and channel sections. At present, the beam element is only applicable to rectangular and tubular cross sections for elastic-plastic material response.

3) The thin shell element in ADINA should be extended to include multilayered and honeycomb cross sections.

4) In general, the ADINA program could be reduced in size by eliminating numerical options, material options, elements and routines that would not be needed for aircraft vulnerability analysis; that is, the program could be tailored for this specific application.

5) The proprietory nature of such a modified ADINA program should be investigated to determine what options are available for a less restricted distribution.

REFERENCES

1. Kaman AviDyne, Handbook for Analysis of Nuclear Weapon Effects on Aircraft, DNA 2048H, KA TR-114, March 1976.

2. Lee, W. N., Mente, L. J., "Nova-2 - A Digital Computer Program for Analyzing Overpressure Effects on Aircraft", Air Force Weapons Laboratory, Kirtland AFB, AFWL-TR-75-262, Parts 1 and 2, August, 1976.

3. Mente, L. J., Lee, W. N., "NOVA-2S - A Stiffened Panel Extension of the NOVA-2 Computer Program", AFWL-TR-78-182, KA TR-153, December 1978.

4. Bathe, K. J., "ADINA, A Finite Element Program for Automatic Dynamic Incremental Nonlinear Analysis," Report 82448-1, Acoustics and Vibration Lab., Mechanical Engineering Dept. MIT (1976).

5. Bathe, K J. and Wilson, E. L., Numerical Methods in Finite Element Analysis, Prentice-Hall, Englewood Cliffs, N.J., 1976.

6. Bathe, K. J., Ramm, E., and Wilson, E. L., "Finite Element Formulations for Large Deformation Dynamic Analysis", Int. J. Num. Meth. Eng., Vol. 9, p. 373, 1975.

7. Bathe, K. J., and Wilson, E. L., "Solution Methods for Eigenvalue Problems in Structural Mechanics", Int. J. Num. Meth. Eng., Vol. 6 1973. pp. 213-266.

8. Bathe, K. J., and Wilson, E. L., "NONSAP - A Nonlinear Structural Analysis Program", Nuclear Eng. and Design, Vol. 29, 1974.

9. Bathe, K. J., Wilson, E. L., and Peterson, F. E., "SAP IV - A Structural Analysis Program for Static and Dynamic Response of Linear Systems", Report EERC 73-11, College of Engineering, University of California, Berkeley, June 1973.

10. Bathe, K. J., "On The Development of Solution Methods for Nonlinear Analysis in Mechanics", Proceedings, Conference on Computer Aids in Manufacturing, Sperry Univac, Nice, France, October 1978.

11. Mente, L. J., Lee, W. N., "DEPROP - A Digital Computer Program for Predicting Dynamic Elastic - Plastic Response of Panels to Blast Loadings", AFATL-TR-76-71, KA TR-133, June 1976.

12. Atluri, S., Witmer, E. A., Leech, J. W., and Morino, L., "PETROS 3: A Finite-Difference Method and Program for the Calculation of Large Elastic-Plastic Dynamically-Induced Deformations of Multilayer Variable-Thickness Shells", BRL CR 60 (MIT-ASRL TR 152-2), November 1971. AD #890200L.

13. Pirotin, S. D., Berg, B. A., and Witner, E. A., "PETROS 3.5: New Developments and Program Manual for the Finite-Difference Calculation of Large Elastic-Plastic Transient Deformations of Multilayer Variable-Thickness Shells", MIT ASRL TR 152-4, October 1973.

14. Witmer, E. A., Balmer, H. A., Theoretical-Experimental Correlation of Large Dynamic and Permanent Deformations of Impulsively-Loaded Simple Structures, Technical Documentary Report No. FDL-TDR-64-108, Air Force Flight Dynamics Laboratory Research and Technology Division, Air Force Systems Command, Wright-Patterson Air Force Base, Ohio, July 1964.

15. Witmer, E. A., Balmer, H. A., Leech, J. W., and Pian, T. H. H., "Large Dynamic Deformations of Beams, Rings, Plates, and Shells", AIAA Journal, Volume I, No. 8, August 1963.

16. Bolourchi, S., Bathe, K. J., "A Geometric and Material Nonlinear Three-Dimensional Beam Element", Report 82448-4, Acoustics and Vibration Lab., Mechanical Engineering Dept., MIT, August, 1977.

17. Bathe, K. J., "Static and Dynamic Geometric and Material Nonlinear Analysis using ADINA," Report 82448-2, Acoustics and Vibration Lab., Mechanical Engineering Dept., MIT (1976).

18. Malvern, L. E., Introduction to Mechanics of a Continuous Medium, Prentice-Hall, Inc., Englewood Cliffs, New Jersey, 1969.

19. Lanczos, Cornelius, The Variational Principles of Mechanics, 4th Ed., University of Toronto Press, Toronto, Ontario, 1977.

20. Wu, R. W-H., and Witmer, E. A., "Finite-Element Analysis of Large Transient Elastic-Plastic Deformations of Simple Structures, with Application to the Engine Rotor Fragment Containment/Deflection Problem", ASRL TR 154-4, Aeroelastic and Structures Research Laboratory, MIT, January 1972 (Available as NASA CR-120886.).

21. Hildebrand, F. B., Introduction to Numerical Analysis, 2nd Ed., McGraw Hill, New York, N.Y., 1974.

22. Ashwell, D. G., Gallagher, R. H., Finite Elements for Thin Shells and Curved Members, John Wiley and Sons, London, 1976.

23. Zienkiewicz, O. C., The Finite Element Method in Engineering Science, McGraw-Hill, London, 1971.

DISTRIBUTION LIST

DEPARTMENT OF DEFENSE

Assistant to the Secretary of Defense
Atomic Energy
ATTN: Executive Assistant

Defense Documentation Center
12 cy ATTN: DD

Defense Intelligence Agency
ATTN: DB-4C, V. Fratzke

Defense Nuclear Agency
ATTN: SPAS
ATTN: STSP
ATTN: DDST
ATTN: SPSS, E. Sevin
ATTN: SPSS, R. Elsbernd
4 cy ATTN: TITL

Field Command
Defense Nuclear Agency
ATTN: FCPR
ATTN: FCT, W. Tyler

Field Command
Defense Nuclear Agency
Livermore Division
ATTN: FCPRL

NATO School (SHAPE)
ATTN: U.S. Documents Officer

Undersecretary of Def. for Rsch. & Engrg.
ATTN: Strategic & Space Systems (OS)
ATTN: M. Atkins

DEPARTMENT OF THE ARMY

BMD Advanced Technology Center
Department of the Army
ATTN: ATC-O, J. Hagestration

Harry Diamond Laboratories
Department of the Army
ATTN: DELHD-N-P
ATTN: DELHD-N-P, J. Gwaltney

U.S. Army Ballistic Research Labs.
ATTN: DRDAR-BLT, W. Taylor

U.S. Army Materiel Dev. & Readiness Cmd.
ATTN: DRCDE-D, L. Flynn

U.S. Army Nuclear & Chemical Agency
ATTN: Library

DEPARTMENT OF THE NAVY

Carderock Laboratory
David Taylor Naval Ship R&D Ctr.
ATTN: Code 1740.5, B. Wang
ATTN: Code 1720, J. Carrado

Naval Air Systems Command
ATTN: Code 320, D. Mulville

DEPARTMENT OF THE NAVY (Continued)

Naval Material Command
ATTN: MAT 08T-22

Naval Research Laboratory
ATTN: Code 2627

Naval Surface Weapons Center
White Oak Laboratory
ATTN: Code F31, K. Caudle

Naval Weapons Evaluation Facility
ATTN: L. Oliver

Office of Naval Research
ATTN: Code 465

Strategic Systems Project Office
Department of the Navy
ATTN: NSP-272

DEPARTMENT OF THE AIR FORCE

Aeronautical Systems Division, AFSC
ATTN: ASD/ENFT, R. Bachman
4 cy ATTN: ASD/ENFTV, D. Ward

Air Force Aero-Propulsion Laboratory
ATTN: TBC, M. Stibich

Air Force Materials Laboratory
ATTN: MBE, G. Schmitt

Air Force Weapons Laboratory, AFSC
ATTN: DYV, A. Sharp
ATTN: SUL
ATTN: DYV, G. Campbell

Assistant Chief of Staff
Studies & Analyses
Department of the Air Force
ATTN: AF/SASB
ATTN: AF/SASC

Deputy Chief of Staff
Research, Development, & Acq.
Department of the Air Force
ATTN: AFRDQSM, L. Montulli

Foreign Technology Division, AFSC
ATTN: SDBF, S. Spring

Strategic Air Command
Department of the Air Force
ATTN: XPFS, B. Stephan

DEPARTMENT OF DEFENSE CONTRACTORS

University of Akron
ATTN: Dept. of Civil Eng., T. Chang

Avco Research & Systems Group
ATTN: J. Patrick
ATTN: P. Grady

DEPARTMENT OF DEFENSE CONTRACTORS (Continued)

BDM Corp.
ATTN: C. Somers

Boeing Co.
ATTN: R. Dyrdahl
ATTN: S. Strack
ATTN: E. York

Boeing Wichita Co.
ATTN: R. Syring
ATTN: K. Rogers

Calspan Corp.
ATTN: M. Dunn

University of Dayton
Industrial Security, Super. KL-505
ATTN: B. Wilt

Effects Technology, Inc.
ATTN: E. Bick
ATTN: R. Parisse
ATTN: R. Wengler
ATTN: R. Globus

General Electric Co.-TEMPO
ATTN: DASIAC

General Research Corp.
Santa Barbara Division
ATTN: T. Stathacopoulos

Kaman AviDyne
Division of Kaman Sciences Corp.
ATTN: N. Hobbs
ATTN: R. Ruetenik
ATTN: E. Criscione
ATTN: J. Stagliana
ATTN: S. Mente

Kaman Sciences Corp.
ATTN: D. Sachs

DEPARTMENT OF DEFENSE CONTRACTORS (Continued)

Los Alamos Technical Associates, Inc.
ATTN: C. Sparling
ATTN: P. Hughes

McDonnell Douglas Corp.
ATTN: J. McGrew

Pacific Technology
ATTN: R. Nickell

Prototype Development Associates, Inc.
ATTN: C. Thacker
ATTN: J. McDonald
ATTN: H. Moody

R & D Associates
ATTN: C. MacDonald
ATTN: J. Carpenter
ATTN: F. Field
ATTN: A. Kuhl

Rockwell International Corp.
ATTN: R. Moonan

Science Applications, Inc.
ATTN: J. Dishon

University of Virginia
ATTN: W. Pilkey

Weidlinger Assoc., Consulting Engineers
ATTN: M. Baron

DEPARTMENT OF ENERGY CONTRACTOR

Sandia Laboratories
ATTN: A. Lieber